



Article

Characterization of the WRKY Gene Family Related to Anthocyanin Biosynthesis and the Regulation Mechanism under Drought Stress and Methyl Jasmonate Treatment in *Lycoris radiata*

Ning Wang^{1,2} , Guowei Song^{1,2}, Fengjiao Zhang^{1,2}, Xiaochun Shu^{1,2}, Guanghao Cheng^{1,2}, Weibing Zhuang^{1,2}, Tao Wang^{1,2}, Yuhang Li^{1,2} and Zhong Wang^{1,2,*}

¹ Institute of Botany, Jiangsu Province and Chinese Academy of Sciences (Nanjing Botanical Garden Mem. Sun Yat-Sen), Nanjing 210014, China

² Jiangsu Key Laboratory for the Research and Utilization of Plant Resources, Jiangsu Provincial Platform for Conservation and Utilization of Agricultural Germplasm, Nanjing 210014, China

* Correspondence: wangzhong@cnbg.net



Citation: Wang, N.; Song, G.; Zhang, F.; Shu, X.; Cheng, G.; Zhuang, W.; Wang, T.; Li, Y.; Wang, Z.

Characterization of the WRKY Gene Family Related to Anthocyanin Biosynthesis and the Regulation Mechanism under Drought Stress and Methyl Jasmonate Treatment in *Lycoris radiata*. *Int. J. Mol. Sci.* **2023**, *24*, 2423. <https://doi.org/10.3390/ijms24032423>

Academic Editor: Maria Lourdes Gómez-Gómez

Received: 7 December 2022

Revised: 7 January 2023

Accepted: 10 January 2023

Published: 26 January 2023



Copyright: © 2023 by the authors. Licensee MDPI, Basel, Switzerland. This article is an open access article distributed under the terms and conditions of the Creative Commons Attribution (CC BY) license (<https://creativecommons.org/licenses/by/4.0/>).

Abstract: *Lycoris radiata*, belonging to the Amaryllidaceae family, is a well-known Chinese traditional medicinal plant and susceptible to many stresses. WRKY proteins are one of the largest families of transcription factors (TFs) in plants and play significant functions in regulating physiological metabolisms and abiotic stress responses. The WRKY TF family has been identified and investigated in many medicinal plants, but its members and functions are not identified in *L. radiata*. In this study, a total of 31 *L. radiata* WRKY (*LrWRKY*) genes were identified based on the transcriptome-sequencing data. Next, the *LrWRKYs* were divided into three major clades (Group I–III) based on the WRKY domains. A motif analysis showed the members within same group shared a similar motif component, indicating a conservational function. Furthermore, subcellular localization analysis exhibited that most *LrWRKYs* were localized in the nucleus. The expression pattern of the *LrWRKY* genes differed across tissues and might be important for *Lycoris* growth and flower development. There were large differences among the *LrWRKYs* based on the transcriptional levels under drought stress and MeJA treatments. Moreover, a total of 18 anthocyanin components were characterized using an ultra-performance liquid chromatography-electrospray ionization tandem mass spectrometry (UPLC-ESI-MS/MS) analysis and pelargonidin-3-O-glucoside-5-O-arabinoside as well as cyanidin-3-O-sambubioside were identified as the major anthocyanin aglycones responsible for the coloration of the red petals in *L. radiata*. We further established a gene-to-metabolite correlation network and identified *LrWRKY3* and *LrWRKY27* significant association with the accumulation of pelargonidin-3-O-glucoside-5-O-arabinoside in the *Lycoris* red petals. These results provide an important theoretical basis for further exploring the molecular basis and regulatory mechanism of WRKY TFs in anthocyanin biosynthesis and in response to drought stress and MeJA treatment.

Keywords: *Lycoris radiata*; WRKY transcription factors; expression patterns; anthocyanin biosynthesis; drought stress; methyl jasmonate treatment

1. Introduction

Transcription factors (TFs) activate diverse signal transduction pathways and modulate the transcriptional mode of targeted genes, which improves plants to adapt to diverse environmental responses [1–4]. Among various TF families, WRKY TFs are one of the largest TF families in plants and play crucial roles in various biological processes, such as physiological metabolism, anthocyanin accumulation, and abiotic stress response [4–6]. WRKY proteins contain a highly conserved WRKY domain (WRKYGQK) at the N-terminus and C2H2 (C-X4-5-CX22-23-H-X-H) or C2HC (C-X7-C-X23-H-X-C) zinc finger motif at the

C-terminus [5]. WRKY proteins can be classified into four main groups (Group I, II, III, and IV) based on the number of WRKY domains and the structure of zinc finger motifs. The Group I members contain two WRKY domains and a C2H2-type zinc finger. The Group II and Group III members have one WRKY domain; Group II members have a C2H2-type zinc finger and the Group III members consist of a C2HC type. The Group IV members contain an incomplete or partial WRKY domain and lack a zinc-finger motif, indicating that this group may have lost their function as WRKY TFs [4,7]. In addition, Group I can be divided into two subgroups, Ia and Ib, based on two WRKY domains at the N and C terminus [7,8]. The Group II WRKY can be further categorized into five subgroups (IIa, IIb, IIc, IId, and IIe) based on the sequence of the DNA-binding domain [8]. Group III is classified into two subgroups (IIIa and IIIb) based on the zinc-finger motif structure [9,10].

The WRKY gene family is widespread in many plants. For example, there are 74 WRKY genes in *Arabidopsis thaliana* [11], 153 WRKY genes in *Brassica napus* L. [12], 88 WRKY genes in *Phaseolus vulgaris* L. [13], 54 WRKY genes in *Ananas comosus* L. [14], 94 WRKY genes in *Sorghum bicolor* L. [15], 44 WRKY genes in *Liriodendron chinense* [16], 138 WRKY genes in *Chrysanthemum lavandulifolium* [17], and 174 WRKY genes in *Arachis hypogaea* L. [18]. Drought is an important abiotic stress factor that prevents plant growth and development and is a regular cause of damage. Many studies have shown that the WRKY TFs play crucial roles in the signaling and regulation of gene expression during drought stress responses [7,19–21]. In a recent study, *GhWRKY21* was found to negatively regulate drought stress responses in cotton [22]. *TaWRKY2*-overexpressing transgenic wheat has been observed to be improved in drought resistance [23]. In *Arabidopsis*, *AtWRKY11*, *AtWRKY17*, *AtWRKY28*, *AtWRKY30*, and *AtWRKY63* have been shown to play positive regulation roles in drought stress responses, while *AtWRKY46*, *AtWRKY54*, and *AtWRKY70* participated in plant growth and play a negative role in drought tolerance regulation [24–28]. Moreover, the overexpression of *GhWRKY1*, *IgWRKY50*, *IgWRKY32*, *MfWRKY41*, *TaWRKY75*, *OsWRKY114*, *ZmWRKY106*, and *TaWRKY133* enhances drought tolerance in transgenic *Arabidopsis* plants [29–36].

The WRKY genes could be up-regulated under methyl jasmonate (MeJA) treatment, suggesting that they are involved in response to abiotic stress, as well as in jasmonic acid (JA) signaling pathways in plants [37]. In *Populus*, most WRKY genes were induced by MeJA and SA treatments [38]. The expression level of *ScWRKY3* in sugarcane was increased under salt, drought stresses, and abscisic acid (ABA) treatment but inhibited by salicylic acid (SA) treatment and MeJA treatment [39]. Differently, the expression level of *ScWRKY5* was induced by salt, drought stresses, as well as SA and ABA treatments [40]. Furthermore, overexpressing *HbWRKY82* of *Hevea brasiliensis* improved drought and salt tolerance and decreased sensitivity to ABA in *Arabidopsis* [41]. Recently, reports have shown that WRKY TFs have a visible correlation with the regulation of anthocyanin biosynthesis. For example, *MdWRKY11* participates in anthocyanin accumulation by affecting *MdMYB* and *MdHY5* in apples [42]. *PyWRKY26* targeted the *PyMYB114* promoter to regulate anthocyanin biosynthesis and transport in red-skinned pears [43]. *PbWRKY75* may promote *PbMYB10b* expression and activate anthocyanin biosynthetic genes *DFR* and *UFGT* to promote anthocyanin accumulation [44]. Moreover, *StWRKY13* could significantly activate anthocyanin biosynthetic genes *StCHS*, *StF3H*, *StDFR*, and *StANS* to promote anthocyanin biosynthesis in potato tubers [45]. In a previous study, *McWRKY71* interacted with *McMYB12* and directly activated *McANR* to participate in the regulation of proanthocyanidin biosynthesis [46]. In apples, *MdWRKY75* mainly activate the promoter of *MdMYB1* and induced the accumulation of anthocyanin [47].

L. radiata is a perennial herbaceous flower with good ornamental characteristics and barren-resistant, water-saving, and drought-resistant properties. Plants in the genus *Lycoris* have been utilized in traditional medicine preparation and more than 110 potent structurally distinct Amaryllidaceae alkaloids were isolated or identified for extensive pharmacological and phytochemical investigations [48]. For example, according to the Compendium of Materia Medica, *Lycoris* plants are described as potent antidotes to poison, effective agents to alleviate pain and relieve inflammation, and diuretic drugs [49]. Amaryllidaceae alkaloids

from *L. radiata* bulbs were traditionally used for treating sore carbuncle, neurodegenerative diseases, poliomyelitis, suppurative wounds, and ulcers [50–52]. In addition, *L. radiata* is an important greening material for energy-saving medicinal construction and a genetic treasure trove for the drought resistant breeding of *Lycoris* and other medicinal plants. Thus, it is of great value for deeply studying the drought resistance of *Lycoris*. At present, amaryllidaceae alkaloid and anthocyanin biosynthesis as well as sucrose degradation have been identified in *Lycoris* plants through transcriptome sequencing [53–58]. In this work, 31 *LrWRKY* genes were identified based on our previous *L. radiata* transcriptome data [53] and their motif pattern and phylogenetic relationship between *Arabidopsis* and *L. radiata* were analyzed. Subcellular localization analysis revealed that these *LrWRKY* proteins were mainly localized in the nucleus. The transcriptome datasets and the qRT-PCR results showed that the expression levels of *LrWRKY* genes changed in different tissues as well as under MeJA treatment and drought stress. To better comprehend the molecular mechanism of petal color formation, we identified *LrWRKYs*, the key structural genes and metabolites that are involved in anthocyanin biosynthesis, combining gene expression and anthocyanin metabolome analyses. Moreover, the probable protein–protein interaction (PPI) of *LrWRKYs* were also predicted. Our results provide important insights into the *LrWRKY* genes in *L. radiata* and lay a foundation for the further investigation of *LrWRKY* genes functioning in the biological pathway.

2. Results

2.1. Identification and Characterization of *LrWRKY* Proteins in *L. radiata*

We used HMMER 3.0 and BLASTP to predict putative *LrWRKY* protein sequences in the *L. radiata* transcriptome database with an E-value threshold of $<1 \times 10^{-5}$. All the candidate sequences were confirmed in NCBI and with SMART to further identify the conserved complete WRKY domains. Thirty-one *LrWRKY* proteins ranged from *LrWRKY1* to *LrWRKY31* were identified and their basic characteristics are shown (Table S1). The coding sequence lengths of *LrWRKY* genes were varied from 459 bp to 1830 bp. The *LrWRKY* proteins ranged from 153 to 610 amino acids in size, from 17.41 to 66.53 kDa in molecular weight, and from 4.80 to 9.83 in their isoelectric points. The subcellular localization of the *LrWRKY* proteins was predicted by using ProtComp 9.0, Plant-mPLoc, and WOLF PSORT. It showed that most of the *LrWRKY* proteins were probably located in the nucleus, and few *LrWRKY* proteins were located in the endoplasmic reticulum and chloroplast. Sixteen *LrWRKY* proteins showed the highest sequence similarity with *Asparagus officinalis* WRKY proteins after homologous alignments. *LrWRKY4* and *LrWRKY24* had the highest sequence similarity with the *Narcissus hybrid* cultivar homologous protein. *LrWRKY13* had the highest sequence identity with the *Narcissus tazetta* subsp. homologous protein.

2.2. Phylogenetic Analysis and Classification of *LrWRKY* Proteins

To investigate the evolutionary relationships of the *LrWRKY* and *Arabidopsis* WRKY (*AtWRKY*) proteins, a phylogenetic tree was constructed (Figure 1). The results showed that 31 *LrWRKY* proteins were clustered into three subfamilies consistent with the tree topology and classification of *AtWRKY* proteins. Meanwhile, *LrWRKY* proteins could be categorized into Group I, Group IIa, Group IIb, Group IIc, Group IId, Group IIe, and Group III. Ten *LrWRKY* proteins were classified as Group I, containing two WRKY domains and one C2H2 zinc-finger motif. A total of 18 *LrWRKY* proteins included one WRKY domain and one C2H2 zinc-binding motif, which were considered to be Group II. Three *LrWRKY* genes were categorized to Group III, consisting of a single WRKY domain and a C2CH zinc-binding motif. According to the *Arabidopsis* WRKY subgroup classification, the *LrWRKYs* in Group II were further subdivided into five subgroups, including groups IIa (1), IIb (2) IIc (6), IId (5), and IIe (4) (Figure 1). These results revealed that WRKY proteins existed in various plant species before their divergence and then independently evolved in each species.

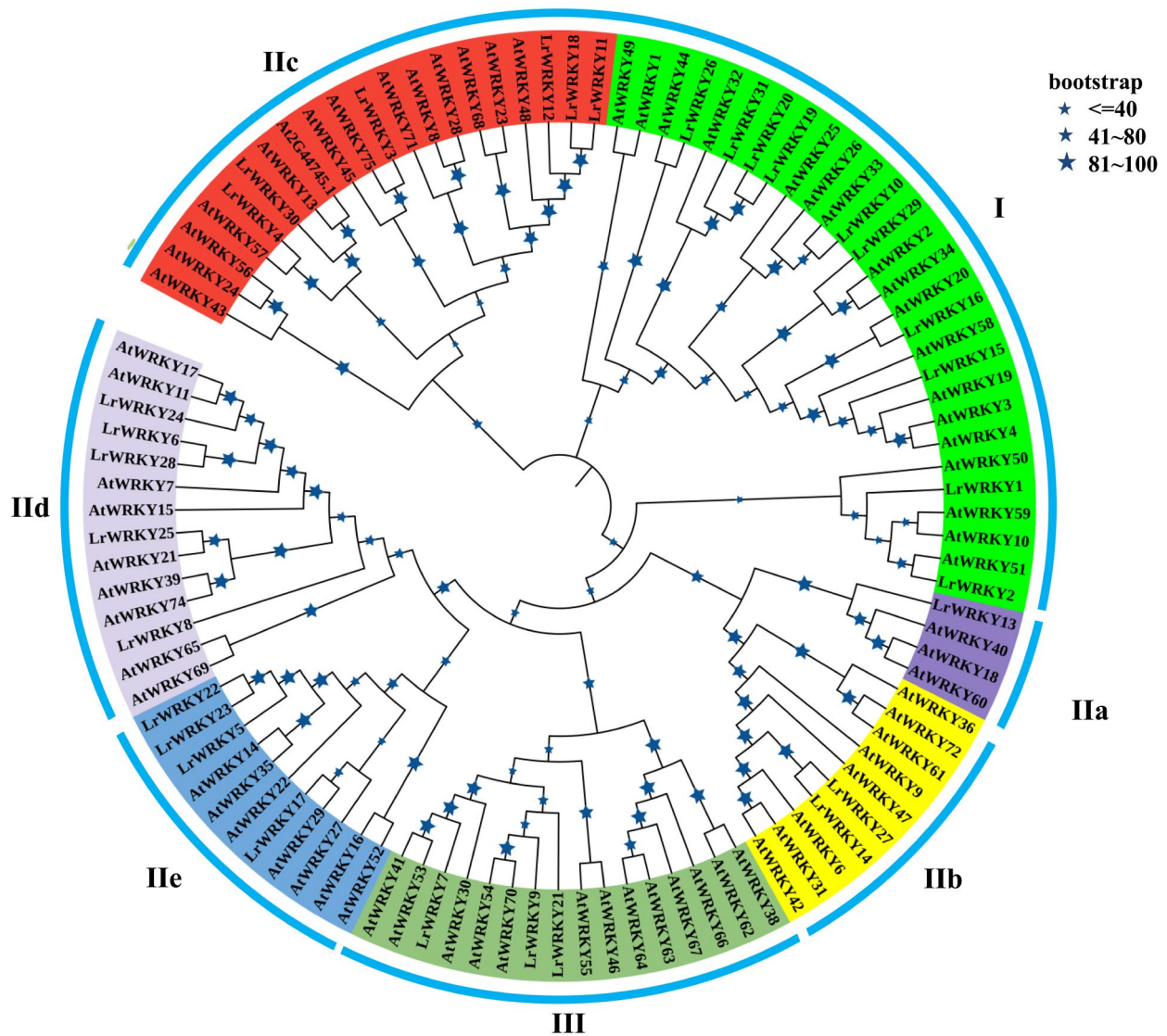


Figure 1. The phylogenetic analysis of *L. radiata* WRKY proteins. The neighbor-joining method was utilized to generate the phylogenetic tree relying on the WRKY domains alignment. These numbers are computed using 1000 bootstrap replicates to verify reliability. The replicate tree percentages indicated with different sizes of asterisk are presented on branches. The tree shows the three subfamilies marked with blue font on a colored background.

2.3. Multiple Sequence Alignment, Conserved Motifs, and WRKY Domains of *LrWRKY* Proteins

To further understand the diversification and conservation of *LrWRKY* proteins, the conservative motifs of *LrWRKY*s were predicted by utilizing MEME software. We found that *LrWRKY* proteins contained a different number of the 10 conserved motifs (Figures 2 and S1). Motif 1 and Motif 2 were the two highly conserved motifs present in most *LrWRKY* proteins except for *LrWRKY*6, *LrWRKY*9, *LrWRKY*11, *LrWRKY*21, *LrWRKY*25, and *LrWRKY*28. The WRKY in the same group contained similar motif structures. Motif 1 and Motif 4 were WRKY domains; Motif 1 was distributed the whole groups, whereas Motif 4 was present in Group I and IIc. Motif 10 was unique to Groups IIa, whereas Motif 8 to Group I and Motif 9 to Group IIe. The clustered *LrWRKY* pairs, such as *LrWRKY*1/2, *LrWRKY*6/28, *LrWRKY*12/18, and *LrWRKY*22/23, displayed a highly similar motif distribution (Figure 2). In addition, the same subgroup of *LrWRKY* proteins has similar motifs, indicating that the protein structure of this family was conserved. The conservative motif arrangement and phylogenetic analysis of the same group proteins can be used as an important basis for categorizing protein.

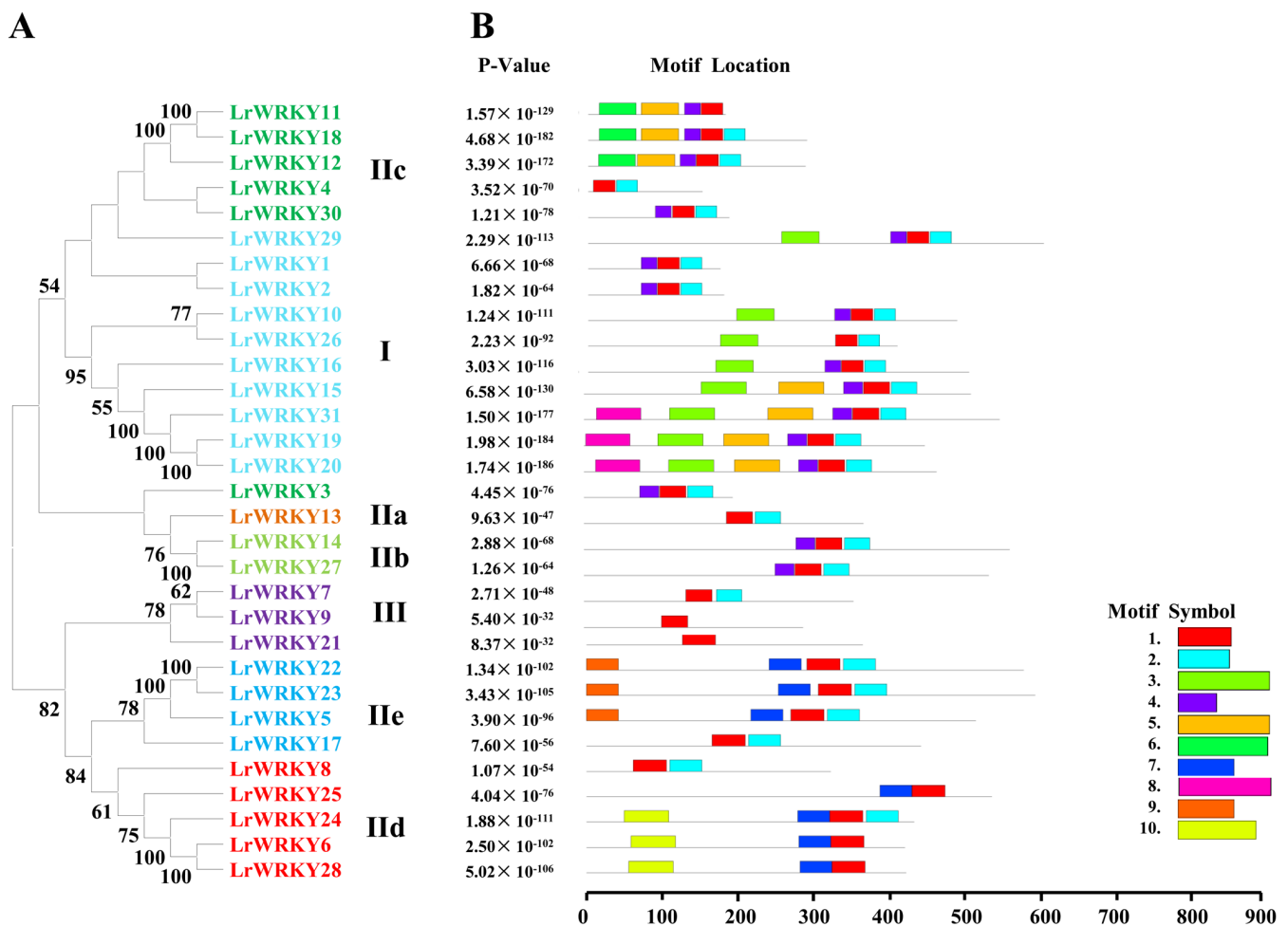


Figure 2. The phylogenetic relationships and conserved motifs analysis of LrWRKY proteins (A) Neighbor-joining LrWRKYs phylogenetic tree (bootstrap values for 1000 replicates); (B) Conserved motif distribution in LrWRKY proteins. Different motifs are represented with different colored boxes. The motif length is represented by the box length.

In addition, conserved amino acids in the WRKY domain analysis via multiple sequence alignments of the LrWRKY proteins were performed (Figure 3). Among the 31 LrWRKY proteins, 9.55% of the proteins have homology in the “WRKYGQK” core domain, which is used for defining classification of the WRKY TFs, while only two proteins (LrWRKY1 and LrWRKY2) have “WRKYGKK” domain (Figure 3). The LrWRKY proteins also had the CX4–7–C–X22–23–H motif, forming C2HC or C2H2 zinc-finger structures.

2.4. Multiple Sequence Alignment, Conserved Motifs, and WRKY Domains of LrWRKY Proteins

To further characterize the functions of LrWRKY TFs, GO annotation and enrichment analysis were performed for all the LrWRKYs. The LrWRKY proteins were annotated to three main GO categories (biological process, cellular component, and molecular function), including 55 biological process terms, nine molecular function terms, and one cellular component terms. The top 20 GO terms of level two were visualized (Figure 4). In biological process terms, 31 LrWRKY proteins were implicated in the regulation of transcription. Most LrWRKYs regulate a defense response to bacterium, response to chitin, defense response to fungus, metal ion binding, regulation of defense response, response to jasmonic acid and SA, as well as response to water deprivation. In cellular component terms, 31 LrWRKY proteins were components of the nucleus. In molecular function terms, 31 LrWRKY proteins were categorized as exhibiting DNA-binding transcription factor activity and sequence-specific DNA binding, respectively (Figure 4).

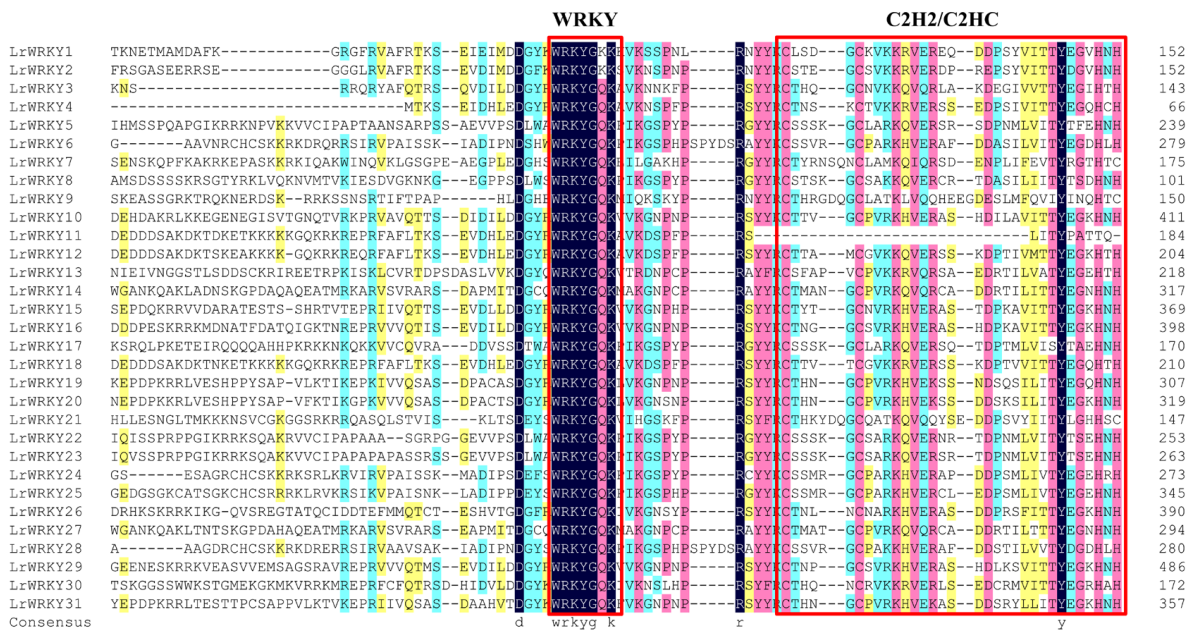


Figure 3. Sequence alignment of 31 LrWRKY proteins. A screenshot of the MEGA X version 10.2.6, showing variation in the conserved domain (WRKYGQK) of LrWRKY proteins and the variation of the conserved domain is encircled in different colors. The yellow boxes indicate 30% identity of amino acids, the blue boxes indicate 50% identity of amino acids, the red boxes indicate 75% identity of amino acids, and the black boxes indicate 100% identity of amino acids.

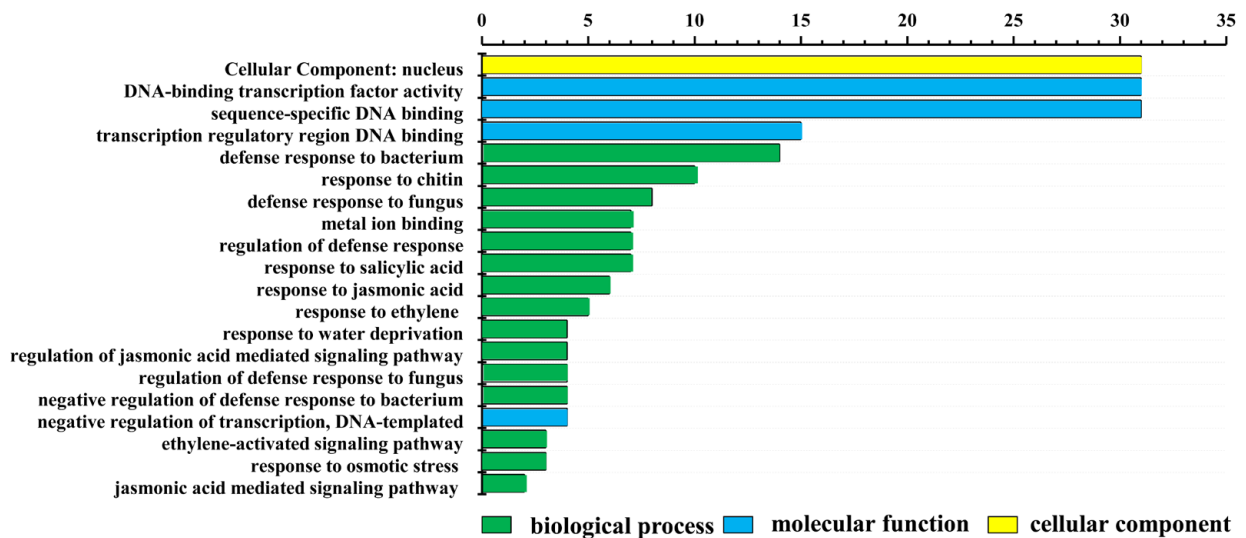


Figure 4. Gene ontology (GO) enrichment analysis of LrWRKY proteins. The top 20 GO terms of level 2 in biological process, cellular component, and molecular function were visualized. The X and Y axes represent the enriched protein numbers and the information on GO terms, respectively.

2.5. Multiple Sequence Alignment, Conserved Motifs, and WRKY Domains of LrWRKY Proteins

As the transcriptome analysis of different tissues (root, leaf, and bulb) has been revealed in *Lycoris longituba* [57], we then searched the orthologous genes of *LrWRKY* by using local blast within *L. longituba* transcriptome data; 31 orthologous genes of *LrWRKY* were found in *L. longituba* (Table S1b). As indicated in Figure S2, some *LrWRKY* genes exhibited differential expressions in the three tissues, whereas other *LrWRKY* genes showed similar expression patterns in diverse tissues. For example, two *LrWRKYs*, including *LrWRKY14* and *LrWRKY27*, were relatively highly expressed in leaves, whereas *LrWRKY22* and *LrWRKY23* were preferentially expressed in roots. *LrWRKY3*, *LrWRKY13*, *LrWRKY16*,

and *LrWRKY30* had the highest relative expression levels in bulb. To further elucidate the biological function of *LrWRKY* proteins, qRT-PCR was utilized to determine the spatial specificity expression pattern of 31 *LrWRKY* genes in eight *L. radiata* organs. As indicated in Figure 5A, some *LrWRKY* genes exhibited differential expression in the eight tissues, whereas other *LrWRKY* genes showed similar expression patterns in diverse tissues, which could be attributed to the functional differentiation of *LrWRKY* genes during plant development. For example, three *LrWRKYs* (i.e., *LrWRKY11*, *LrWRKY12*, and *LrWRKY17*) were relatively highly expressed in leaves. *LrWRKY22* and *LrWRKY23* were preferentially expressed in petals. *LrWRKY29* showed high expression levels in gynoecium, whereas *LrWRKY30* had relatively high expression levels in bulb. In addition, five *LrWRKYs* (i.e., *LrWRKY2*, *LrWRKY5*, *LrWRKY13*, *LrWRKY16*, and *LrWRKY19*) were highly expressed in stamens tissues. In particular, *LrWRKY4*, *LrWRKY6*, *LrWRKY10*, *LrWRKY18*, *LrWRKY24*, and *LrWRKY31* were predominantly expressed in roots. *LrWRKY15* was relatively highly abundant in seeds. *LrWRKY1* and *LrWRKY25* had the highest relative expression levels in flower stalks. Among all the tissues, the fewest *LrWRKY* members were expressed the most in the roots and leaves. Conversely, some genes were not expressed specifically. We noticed that similar expression patterns for *LrWRKY7*, *LrWRKY9*, *LrWRKY10*, *LrWRKY24*, *LrWRKY28*, and *LrWRKY31* in different tissues suggest possible redundancy. These results suggested that *LrWRKYs* might play important functional roles in the growth and development of *L. radiata*.

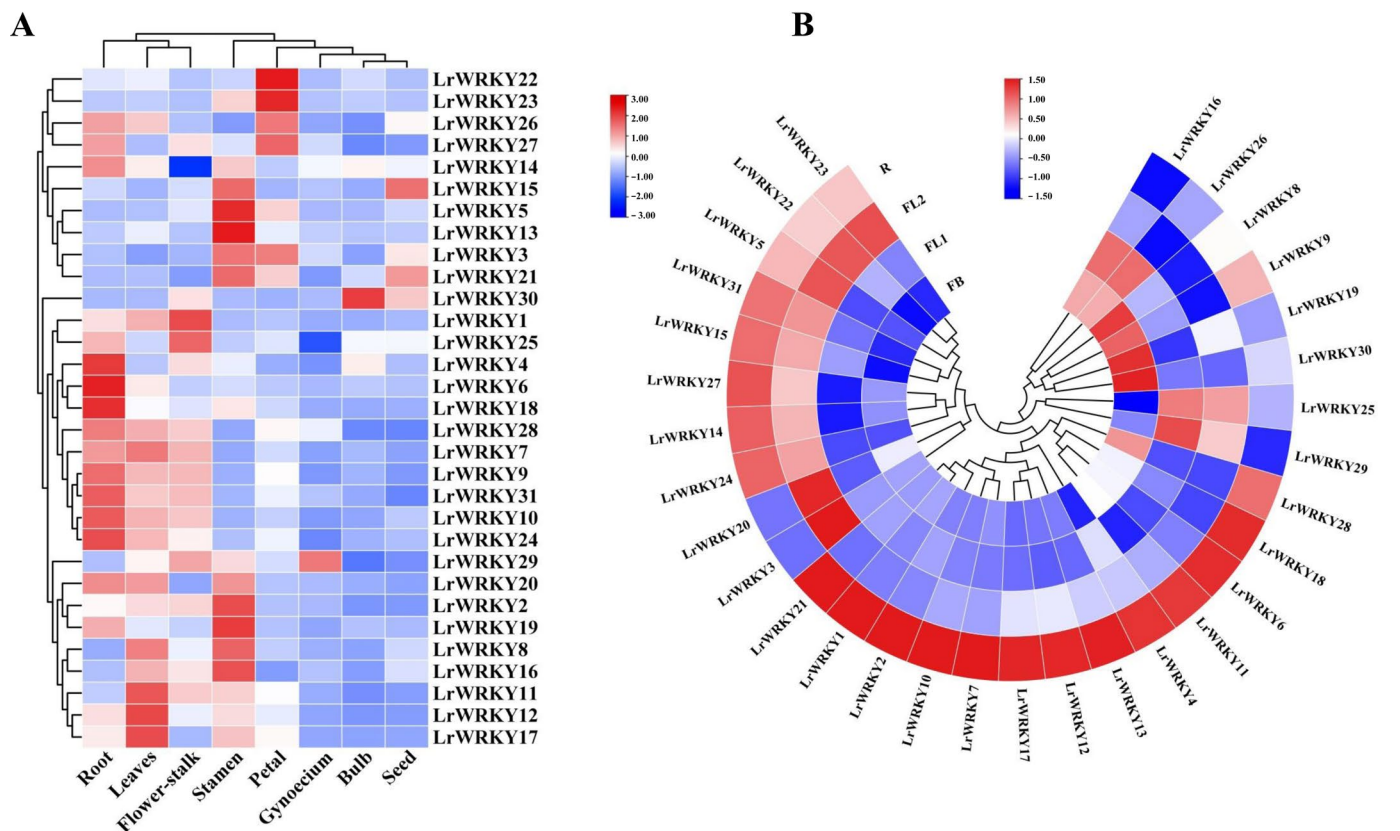


Figure 5. *LrWRKY* gene expression patterns in various *L. radiata* tissues. (A) Expression profile heatmap with hierarchical clustering of *LrWRKYs* in different tissues of *L. radiata*. (B) Expression profile heatmap with hierarchical clustering of *LrWRKYs* at different flower developmental stages of *L. radiata*. The relative expression for each gene is depicted by color intensity in each field. Higher values are represented by red, whereas lower values are represented by blue. FB, flower—bud differentiation stage; FL1, partially opening flower stage; FL2, fully opened flower stage; R, senescent flower stage.

On the basis of tissue-specific expression, the expression of *LrWRKYs* was further observed at the flowering developmental stages using previously published RNA-seq data

(Figure 5B). In *L. radiata* flowering development, FB, FL1, FL2, and R indicated the initial stage of flower—bud differentiation, partially opening flower, fully opened flower, and senescent flower stage, respectively (Figure 5B). Over half of the *LrWRKY* genes were expressed lower at the FB stage and then markedly increased at the R stage. In addition, the expression of *LrWRKY15* and *LrWRKY31* exhibited a gradual increase during flower development. Remarkably, the expression of *LrWRKY16* and *LrWRKY26* genes exhibited opposite trends in the flowering developmental stages, indicating they may perform diverse functions. However, the expression of *LrWRKY8*, *LrWRKY9*, *LrWRKY19*, and *LrWRKY30* were relatively higher at the early stages of flower development.

2.6. Expression Patterns of *LrWRKYs* in Response to Drought Stress and MeJA Treatment

We subsequently examined the gene expression profiles of *LrWRKY* in the roots and leaves of one-year-old *L. radiata* seedlings that were subjected to drought stress for 24 h. As shown in Figure 6A, the responses of *LrWRKYs* were different between individuals after drought treatment. In the *L. radiata* leaves and roots, the majorities of *LrWRKY* genes were down-regulated and showed statistically significant higher expression patterns after 24 h of drought stress compared to the control (Figure 6A). Nonetheless, the expression of *LrWRKY5*, *LrWRKY22*, and *LrWRKY23* reached the highest level under drought stress in *L. radiata* roots. Moreover, the expression levels of *LrWRKY2*, *LrWRKY6*, *LrWRKY28*, *LrWRKY30*, and *LrWRKY31* genes gradually down-regulated after drought stress in *L. radiata* roots. In the *L. radiata* leaves, *LrWRKY4* and *LrWRKY8* were significantly up-regulated under drought treatment. Besides, the expression levels of *LrWRKY1*, *LrWRKY9*, *LrWRKY16*, *LrWRKY19*, *LrWRKY20*, *LrWRKY21*, *LrWRKY25*, and *LrWRKY26* gradually down-regulated under drought treatment in leaves (Figure 6A). These results suggest that *LrWRKY* genes regulate plant physiological processes.

Previous study of *Lycoris aurea* transcriptome sequencing has revealed that MeJA treatment could induce the expression of *LaWRKY* genes [54]. Thus, the orthologous genes of *LrWRKY* in *L. aurea* transcriptome data were also searched. All the 31 *LrWRKY* genes were found to have orthologous transcripts in *L. aurea* transcriptome (Table S1). Among them, eight homologous *LrWRKYs* were up-regulated, while nine homologous *LrWRKY* genes were suppressed with MeJA treatment for 6 h (Figure S3). In addition, homologous genes of *LrWRKY5* and *LrWRKY17*, *LrWRKY15*, and *LrWRKY16* exhibited no expression changes after MeJA treatment. Further, the expression patterns of the *LrWRKYs* tested using qRT-PCR and most *LrWRKYs* expression levels were up-regulated by MeJA treatment and varied over time (Figure 6B). The transcription level of *LrWRKYs* was up-regulated after 6 h, whereas it was down-regulated at 12 h. Specifically, the expression levels of nine genes (*LrWRKY6*, *LrWRKY11*, *LrWRKY12*, *LrWRKY13*, *LrWRKY15*, *LrWRKY18*, *LrWRKY24*, and *LrWRKY28*) increased rapidly under MeJA treatment, while those of the other ten genes (*LrWRKY5*, *LrWRKY8*, *LrWRKY16*, *LrWRKY19*, *LrWRKY20*, *LrWRKY22*, *LrWRKY23*, *LrWRKY25*, *LrWRKY26*, and *LrWRKY31*) were lower under MeJA treatment than that in the control. In addition, the expression profiles of some genes changed dramatically in specific time. For instance, the expression performance of *LrWRKY7* and *LrWRKY9* at 24 h were lower than those in the control but were significantly unregulated at 36 h. The expression trends of *LrWRKY10*, *LrWRKY11*, *LrWRKY14*, and *LrWRKY22* were consistent with the transcriptome data. There were certain divergences between the actual examined and transcriptome data, which can be demonstrated by the individual divergences between the material transcriptome data and the qRT-PCR analysis. In particular, the expression pattern of *LrWRKY6*, *LrWRKY12*, *LrWRKY18*, and *LrWRKY28* up-regulated rapidly at 6 h. After 24 h of MeJA treatment, the expression pattern of *LrWRKY17* and *LrWRKY21* up-regulated rapidly. From these data, it can be speculated that MeJA regulates the expression pattern of the *LrWRKY* genes. These findings revealed that *LrWRKYs* displayed different expression patterns in response to MeJA hormone treatment and potentially participated in developmental processes via hormone signaling pathways in *Lycoris*.

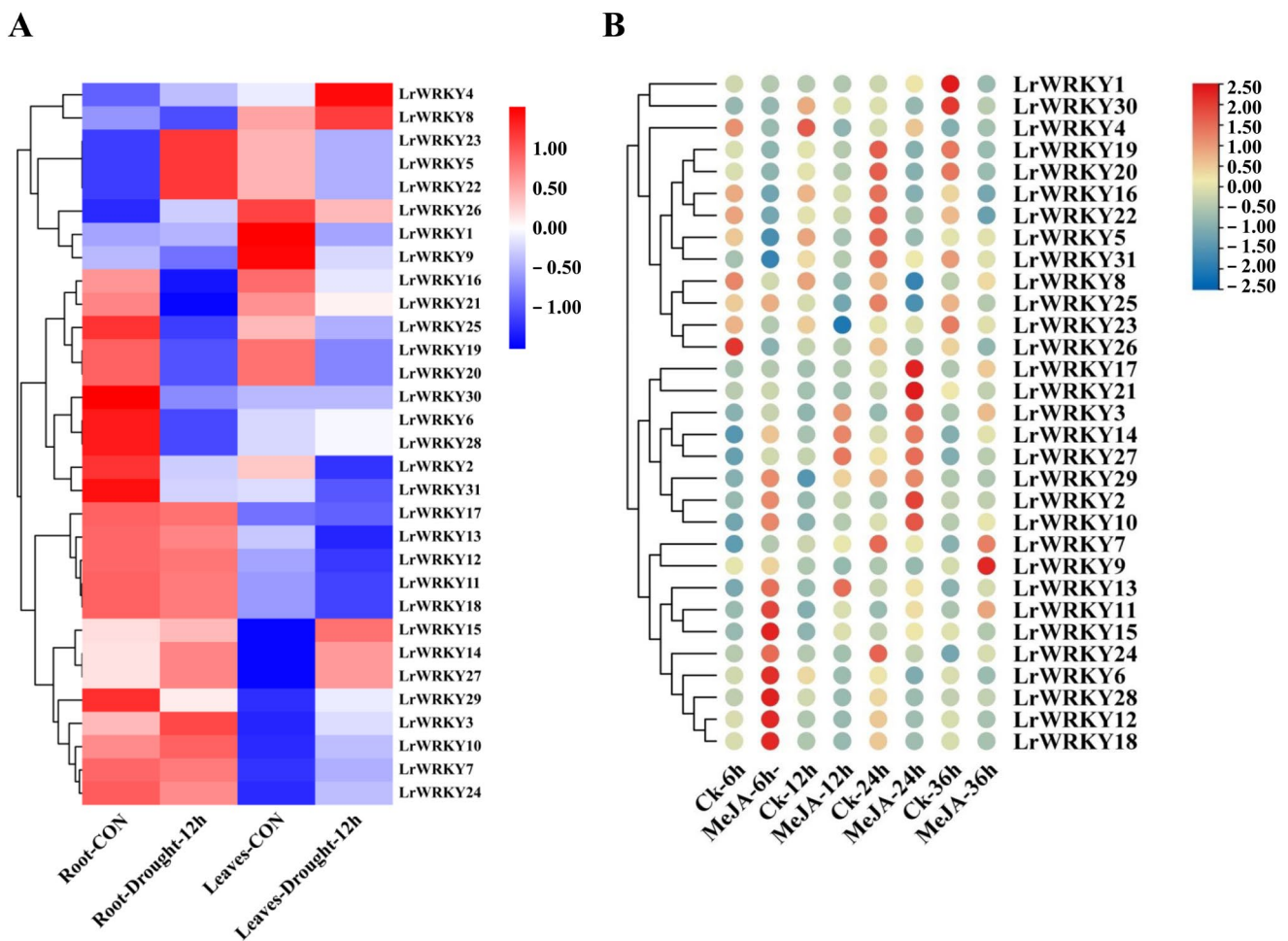


Figure 6. *LrWRKY* gene expression profiles under drought stress and MeJA treatment in *L. radiata*. (A) Heatmap with hierarchical cluster analysis of drought-responsive differentially expressed *LrWRKY* genes. (B) Heatmap of *LrWRKY* genes expression profiles with MeJA treatment. Red and blue represent high and low relative transcript abundance, respectively.

2.7. Identification of the Main Anthocyanin Pigments in *L. radiata* Petals

To detect the metabolic mechanism of the red petal color phenotype in *L. radiata*, the total anthocyanins in the petals were measured [53]. To further ascertain the metabolic mechanism of the *L. radiata* petals, the anthocyanin metabolites were detected using UHPLC-ESI-MS/MS; 18 anthocyanin compounds were identified and quantified in the *L. radiata* petals (Figure 7A). We found that the pelargonidin-3-O-glucoside-5-O-arabinoside content was the highest in the *L. radiata* petals, followed by Cyanidin-3-O-sambubioside (Figure 7A). Given that these two compounds may play a key role in red petal color formation in *L. radiata*, we propose that these anthocyanins were the main compounds responsible for the red coloration of petal margins.

2.8. Integrating Related *LrWRKY* Genes and Metabolites in Anthocyanin Biosynthesis Pathway

WRKY TFs are important regulators of anthocyanin accumulation and they characteristically act by controlling the structural gene expression in the anthocyanin biosynthesis pathway. To enunciate the relationship between *LrWRKYs* and anthocyanin biosynthesis in *L. radiata*, we established a co-expression network of *LrWRKYs* and the anthocyanin metabolites (Figure 7B,C and Table S2). The PCC between the expression performance of *LrWRKYs* and the anthocyanin metabolites was further calculated. The results implied that eight *LrWRKYs* (*LrWRKY1*, *LrWRKY3*, *LrWRKY6*, *LrWRKY7*, *LrWRKY13*, *LrWRKY15*, *LrWRKY17*, and *LrWRKY27*) positively regulated the anthocyanin metabolites, whereas

four *LrWRKYs* (*LrWRKY16*, *LrWRKY22*, *LrWRKY25*, and *LrWRKY29*) negatively regulated the anthocyanin metabolites. Furthermore, pelargonidin-3-O-glucoside-5-O-arabinoside was strongly correlated with the expression of *LrWRKYs*, indicating that pelargonidin-3-O-glucoside-5-O-arabinoside play a significant role in the red petal color in *L. radiata*. Among these *LrWRKYs*, the expression level of *LrWRKY3* and *LrWRKY27*, indicated a remarkable positive correlation with the pelargonidin-3-O-glucoside-5-O-arabinoside content in the samples (PCC > 0.9, Figure 7B,C and Table S2), suggesting that *LrWRKY3* and *LrWRKY27* may have an essential role in the pelargonidin accumulation.

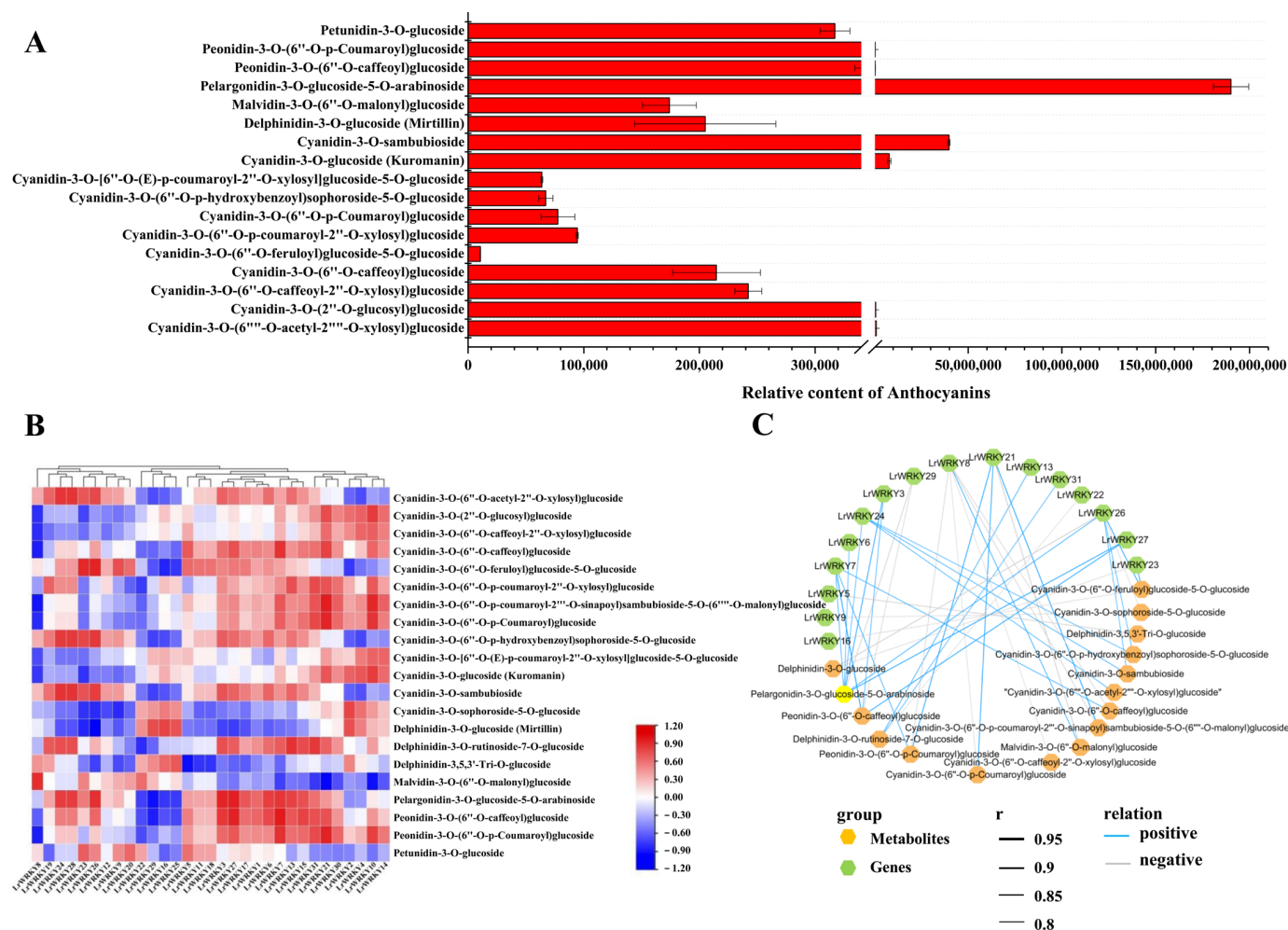


Figure 7. The regulatory network of key anthocyanins metabolites and *LrWRKY* genes in *L. radiata*. (A) Eighteen anthocyanins were identified and quantified from petals of *L. radiata*. (B) The Pearson's correlation coefficients of *LrWRKYs* with an anthocyanin biosynthesis pathway in *L. radiata*. Higher values are represented by red, whereas lower values are represented by blue. (C) Correlation network of metabolite-related *LrWRKY* genes involved in anthocyanin biosynthetic pathways. *r* represents the Pearson correlation coefficient; relation represents the correlation, including positive ($r > 0.8$) and negative correlations ($r < -0.8$).

The correlation between *LrWRKYs* and differently expressed genes (DEGs) of anthocyanin biosynthesis in *L. radiata* could be divided into three main clusters (Figure 8A and Table S3). In Cluster II, several *LrWRKY* genes (*LrWRKY1*, *LrWRKY3*, *LrWRKY5*, *LrWRKY7*, *LrWRKY13*, *LrWRKY15*, *LrWRKY17*, *LrWRKY24*, *LrWRKY26*, and *LrWRKY27*) showed strong correlations with *phenylalanine ammonia lyase* (*PAL*), *cinnamate 4-hydroxylase* (*C4H*), *chalcone synthase* (*CHS*), *dihydroflavonol reductase* (*DFR*), *flavonoid 3'-hydroxylase* (*F3'H*), and *leucoanthocyanidin reductase* (*LAR*) genes in the anthocyanin pathway. In contrast, the *LrWRKYs* in Cluster I showed a low correlation with anthocyanin biosynthetic pathway genes

in *L. radiata* and only correlated strongly with upstream one *PAL* and one *4-coumarate:CoA ligase (4CL)* genes. Some *LrWRKYs* in Cluster III showed a strong negative correlation with the pathway genes. The co-expression analysis showed that the anthocyanin pathway genes were relevant to *LrWRKYs* in Cluster II and that *LrWRKY3*, *LrWRKY7*, *LrWRKY26*, and *LrWRKY27* were selected for their modulatory potential in anthocyanin biosynthesis. In particular, we observed that the identified anthocyanin biosynthesis DEGs and key transcription factors were significantly correlated with nine anthocyanins, including Pelargonidin-3-O-glucoside-5-O-arabinoside, Malvidin-3-O-(6''-O-malonyl) glucoside, Delphinidin-3,5,3'-Tri-O-glucoside, Delphinidin-3-O-glucoside, Cyanidin-3-O-(6''-O-p-Coumaroyl) glucoside, Cyanidin-3-O-(6''-O-p-coumaroyl-2'''-O-sinapoyl)sambubioside-5-O-(6'''-O-malonyl) glucoside, Cyanidin-3-O-(6''-O-feruloyl) glucoside-5-O-glucoside, Peonidin-3-O-(6''-O-p-Coumaroyl) glucoside, and Peonidin-3-O-(6''-O-caffeoyl) glucoside (Figure 8B and Table S3). Some crucial *LrWRKYs* involved in anthocyanin biosynthesis, such as *LrWRKY3*, *LrWRKY7*, *LrWRKY21*, *LrWRKY26*, *LrWRKY27*, and *LrWRKY28* were positively related to the accumulation of nine anthocyanins and anthocyanin enzyme-encoding DEGs including *anthocyanidin synthetase (ANS)*, *4CL*, *CHS*, *C4H*, *chalcone isomerase (CHI)*, *DFR*, *F3'H*, *LAR*, and *PAL*. These results revealed that the *LrWRKY* genes and anthocyanin biosynthesis genes might be involved in the petal red color in *L. radiata*.

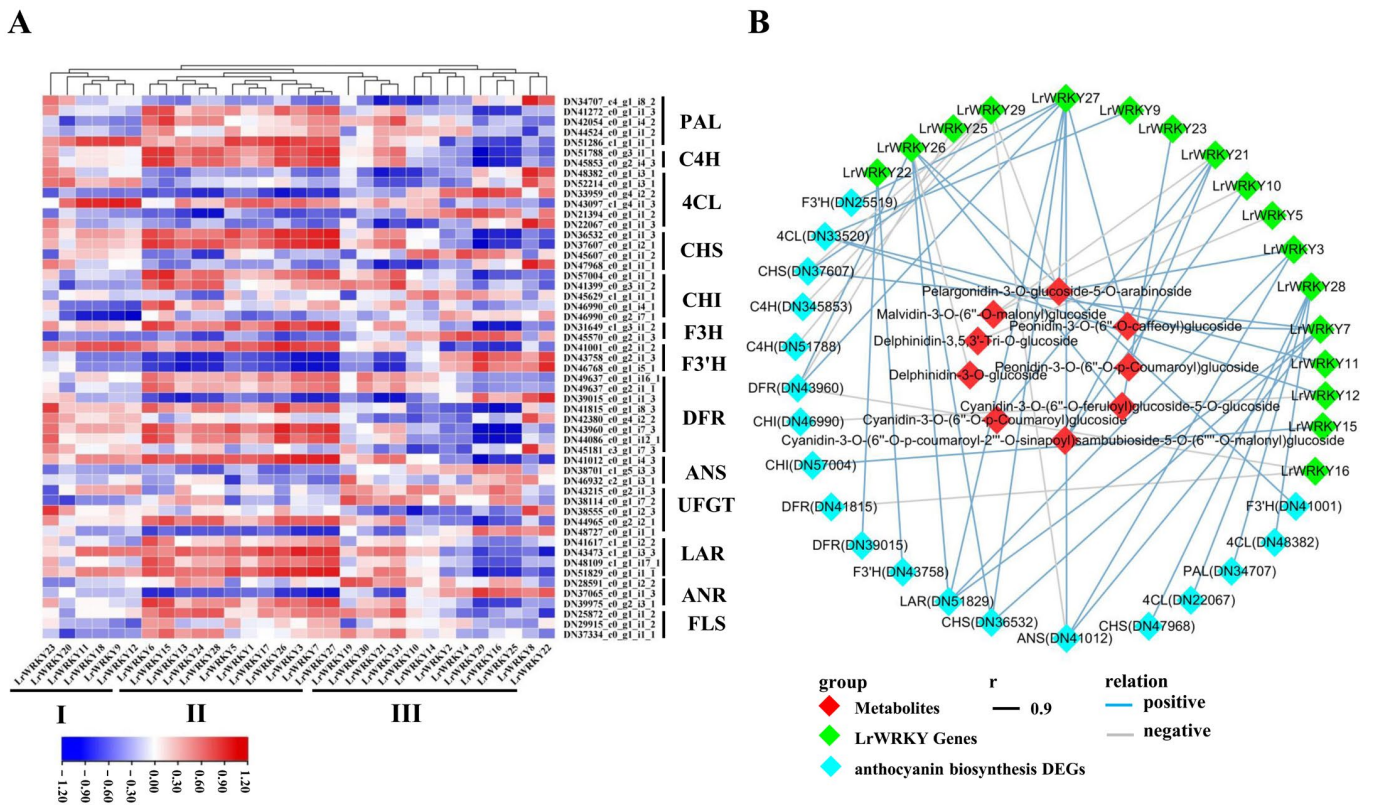


Figure 8. The regulatory network of key differently expressed genes (DEGs) of anthocyanin biosynthesis, metabolites, and *LrWRKY* genes in *L. radiata*. **(A)** The Pearson's correlation coefficients of *LrWRKYs* with DEGs of anthocyanin biosynthesis in *L. radiata*. The enzymes include cinnamate 4-hydroxylase (C4H), 4-coumarate:CoA ligase (4CL), phenylalanine ammonia lyase (PAL), chalcone synthase (CHS), flavone 3-hydroxylase (F3H), chalcone isomerase (CHI), flavonoid 3'-hydroxylase (F3'H), dihydroflavonol reductase (DFR), flavonol synthase (FLS), UDP-flavonoid glucosyl transferase (UFGT), anthocyanidin synthetase (ANS), anthocyanidin reductase (ANR), and leucoanthocyanidin reductase (LAR). **(B)** Correlation network of metabolite-related *LrWRKY* genes and DEGs involved in anthocyanin biosynthetic pathways. r represents the Pearson correlation coefficient; relation represents the correlation, including positive ($r > 0.9$) and negative correlations ($r < -0.9$).

2.9. PPI Networks of LrWRKY Proteins

Based on the orthologs of *Arabidopsis* (Table S4), the STRING database predicted that numerous LrWRKY proteins associate with each other (Figure 9; Table S5), suggesting that the WRKY proteins binding activity is based on the homodimer or heterodimer formation among WRKY proteins [59]. Generally, we predicted several key interactions (Figure 9, Table S5). We identified eight high-confidence interacting proteins in the *Arabidopsis* WRKY family: ACS6 (aminocyclopropane-1-carboxylic acid synthase 6) and GUN5 (genomes uncoupled 5) proteins involved in abiotic stress responses; MPK1 (mitogen-activated protein kinase 1), MPK3, and MPK4 proteins involved in plant responses to pathogens and stresses; and VQ motif-containing (VQ) proteins such as MKS1 (Meckel syndrome, type 1), SIB1 (sigma factor binding protein 1), and SIB2 involved in regulating plant defense responses. In addition, the LrWRKY10 is highly homologous to *Arabidopsis* WRKY33, indicating that it may have potentially stronger interactions with most plant defense proteins (MPK3, MPK4, MKS1, and SIB1). Similarly, the LrWRKY13, LrWRKY21, and LrWRKY27 protein is highly homologous to *Arabidopsis* WRKY40, WRKY70, and WRKY6, which are presumed to have a strong interaction with the internal members of the WRKY family. These findings partially validate the anticipated interaction networks and suggest that they may have comparable roles in *L. radiata*.

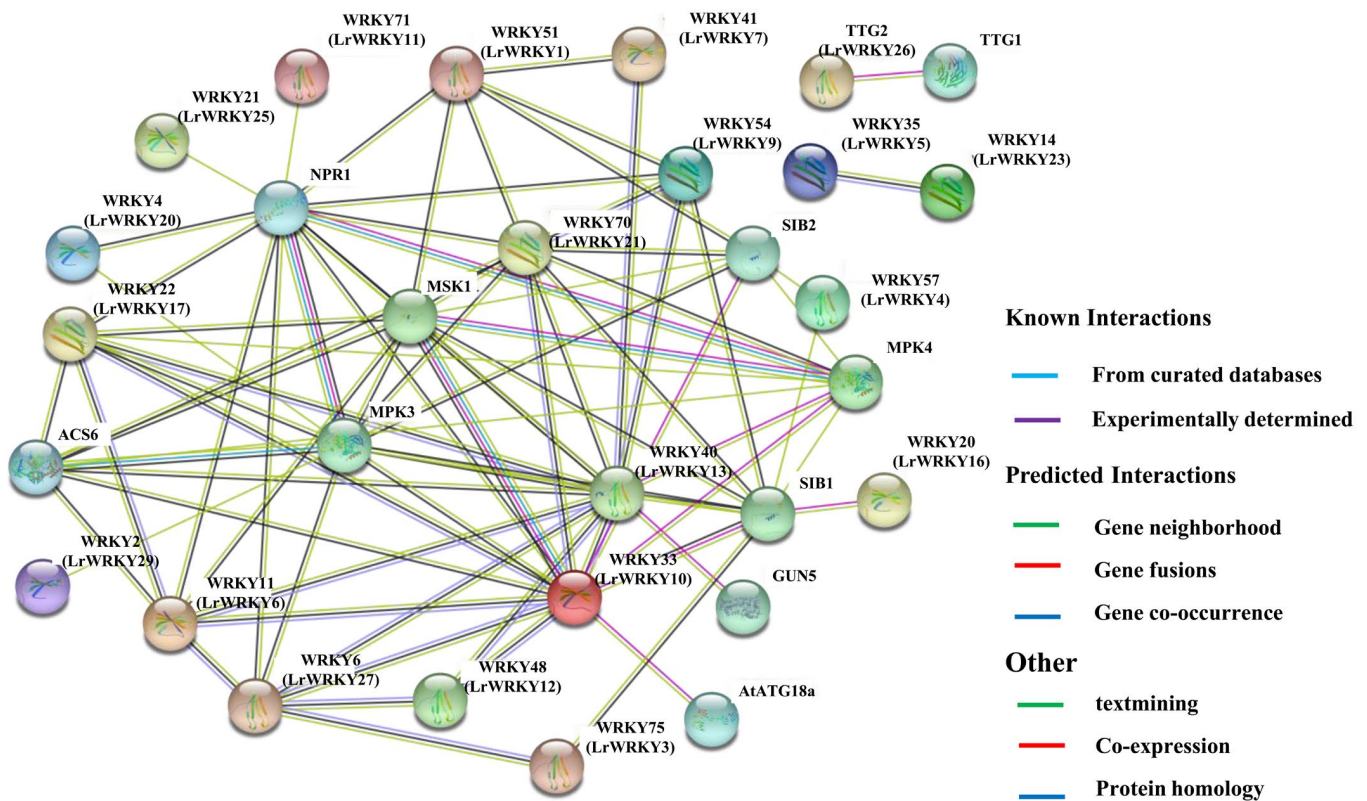


Figure 9. The predicted network of protein–protein interactions between LrWRKYs using the STRING database. Different colors represent different interaction types. *Arabidopsis* WRKY names are marked, whereas their homologs in *L. radiata* are in parentheses.

2.10. Subcellular Localization of LrWRKY Proteins

Based on prediction analysis, most LrWRKY proteins were predicted as localized in the nucleus, whereas few of the LrWRKYs were located in the chloroplast and/or endoplasmic reticulum (Table S1). Subsequently, certain LrWRKY proteins fused to GFP were transiently expressed in *N. benthamiana* epidermal cells using 35S-GFP construct as a positive vector to validate their subcellular localization. The results confirmed that LrWRKY3, LrWRKY10, LrWRKY13, LrWRKY21, and LrWRKY27 proteins were localized in the nucleus (Figure 10).

Thus, these fluorescent microscopy data confirm that most LrWRKYs are nucleoproteins based on their targeting and translocation to the nucleus.

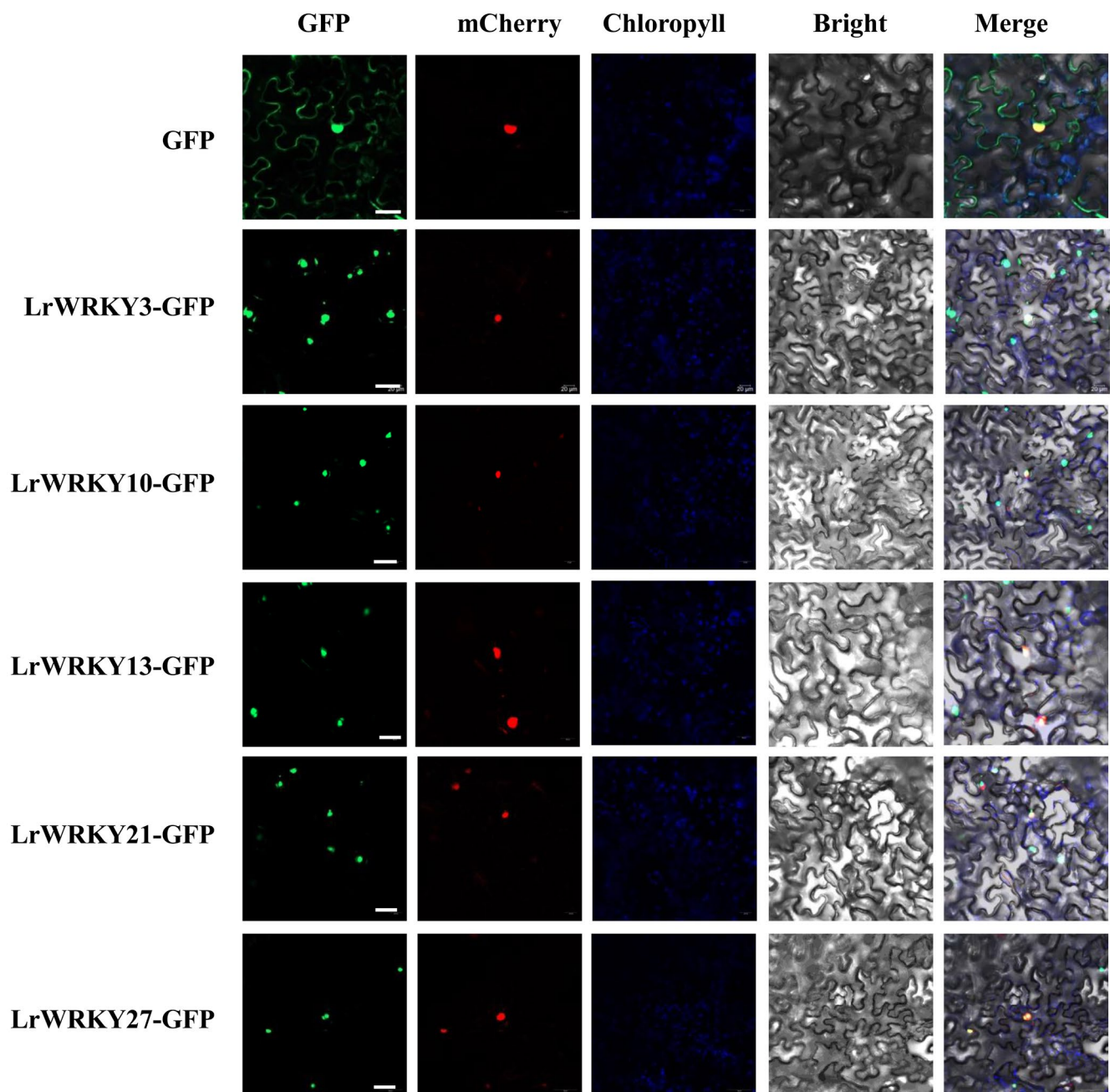


Figure 10. Subcellular localization of LrWRKYs with GFP as a control, which were transiently expressed in *N. benthamiana* leaves. The photographs were taken using the green channel (GFP fluorescence), red channel (nuclear marker protein AtCOL), blue channel (chlorophyll represents chlorophyll auto fluorescence), bright channel, and their combination under a confocal microscope. Merged bright-field, green fluorescence, red fluorescence, blue fluorescence, and green—red—blue fluorescence images. Scale bar = 10 μ m.

3. Discussion

3.1. Characterization of the WRKY Gene Family in *L. radiata*

In plants, WRKY TFs are one of the largest transcription families, playing an important role in plant physiological processes, diverse biotic and abiotic stress responses, and secondary metabolite synthesis in different crop species, including *Arabidopsis*, Chinese

cabbage, peanut, pepper, rice, and tomato [5,7,8,18,60–64]. WRKY TF families have been reported in many plants, but little is known concerning the functions of the WRKY TF in *L. radiata*. In this study, we identified 31 *LrWRKY* genes through homolog search and domain analysis utilizing previously published transcriptome data (Table S1; [53]). The *LrWRKYs* had similar properties in terms of the encoding amino acids number, isoelectric point, and motifs to WRKYs in *A. thaliana* and other plants [62]. In our research, we combined the phylogeny analysis with full-length protein sequences and the classification of *Arabidopsis* WRKY groups to categorize the WRKY groups in *L. radiata* [10]. Generally, highly conserved WRKYs will group together and perform similar or identical molecular functions, pertaining to the same WRKY group (Figure 1). In general, the WRKY proteins of *L. radiata* classified into three groups (containing Group I, Group II (II-a, II-b, II-c, II-d, II-e), and Group III) contingent on the conserved types of WRKY domains and their zinc-finger domains, which were similar to other plants [60–64].

Previous studies proposed four main WRKY TF lineages in flowering plants, namely Group I + IIc, Group IIa + IIb, Group II d + IIe, and Group III, which accurately reflected the evolution of the WRKY TF family members (Figure 1; [65]), which was also verified for *L. radiata*. For example, the Group IIa members and Group IIb members were in the same evolutionary branch and the Group II d members and Group IIe members were grouped into the same branch, suggesting that these subgroups arose indirectly from a common ancestor. Out of the 31 members, 29 were properly conserved in the “WRKYGQK” domain. The substitution of glutamine occurs instead of lysine in two WRKY heptapeptide domains (Figure 3). This “WRKYGKK” domain sequence is reported to be a major variant in many studies [60–66]. The mutation in the WRKYGQK conserved domain mainly occurs from “Q” to “K” amino acid. For example, *LrWRKY1* and *LrWRKY2* replaced “Q” by “K” as their respective domains were also reported in *Camelina sativa* [66]. The same kind of substitution was observed in the WRKY gene family of *Chrysanthemum lavandulifolium* [17]. The motif of *LrWRKY* genes on the same branch commonly has a similar domain component. These results can be used as an important basis for WRKY protein classification (Figure 2). These motifs are associated with transcriptional activity and protein–protein interactions of target genes [67]. Therefore, the characterizations and functions of *LrWRKY* TFs can be appraised by analyzing conserved motif information. All the *LrWRKYs* had more than two conserved motifs, coincident with other plant species reports [68,69]. Each group member had the same or similar motif constitute, suggesting that the same group WRKY TFs have same or similar protein structures and biological functions.

3.2. The WRKY Gene Expression Patterns Facilitate Their Functional Analysis

We methodically analyzed the expression patterns of *LrWRKY* TFs in various tissues to investigate their physiological role in *L. radiata* biological processes. The homologous genes with similar expression profiles are conserved due to the dosage effect, whereas the homologous genes with different expression profiles are retained by functionalization and subfunctionalization [70]. We used transcriptome data from different tissues of two *Lycoris* species to determine the WRKY family gene expression (Figures 5 and S2). In the present study, the *LrWRKYs* of *Lycoris* were expressed differentially in the leaves, roots, flowers, and stems. The WRKY TF genes play an important role in plant development. This indicated that *LrWRKYs* play a critical role in the growth and development of *Lycoris*. The *LrWRKY* genes were expressed in at least one tissue and their expression patterns varied markedly among the different tissues. As shown in Figure S2, the *LrWRKY* genes in roots were higher than those in the leaves and bulb. This study also analyzed the differences in eight tissues of *L. radiata* (Figure 5A). Notably, six *LrWRKY* genes displayed the highest expression patterns in roots. Three *LrWRKY* genes were highly expressed in the leaves, whereas one *LrWRKY* gene was highly expressed in the gynoecium, or seed, or bulb. Five *LrWRKY* genes and two *LrWRKYs* genes were highly expressed in stamens and in flower-stalk tissues, respectively. These tissue-specific expression patterns propose that *LrWRKYs* may be involved in *Lycoris* tissue-specific developmental and signal transduction

processes. As reported, the *AtWRKY70* gene has significantly contributed to *Arabidopsis* root development. The experimental results proclaimed that the *wrky70* mutant had longer roots than the wild type [28,71]. Similarly, the orthologous protein of *AtWRKY70*, named *LrWRKY21*, was specifically expressed in the roots (Figure 5A). This research indicated *LrWRKY21* may be involved in regulating the *L. radiata* roots growth and development. Moreover, *AtWRKY75* also regulate the early accumulation of anthocyanin and increase the length and number of lateral roots and root hairs [72]. The *LrWRKY3* was orthologous genes of *AtWRKY75*, which has difference expression levels in roots and flower (Figure 5). These results displayed the significant contribution of *LrWRKY3* and *LrWRKY21* in the development of roots. Moreover, *LrWRKY29* is significantly expressed in the gynoecium at the *L. radiata* flowering stage and has a close homology with *Arabidopsis AtWRKY2*, suggesting that *LrWRKY29* play an important role in the flowering stage of *Lycoris*, as *Arabidopsis* homologs gene *AtWRKY2* are the key regulators of pollen development [73].

In addition to playing a momentous role in plant development, the WRKY TFs also play critical roles in plant abiotic stress responses [21]. In the present research, *AtWRKY75* gene facilitates leaf senescence and flowering in *Arabidopsis* [74,75]. A recent study showed that *PdeWRKY75*, which is orthologous with *AtWRKY75*, is involved in the manipulation of multiple biological processes by regulating hydrogen peroxide content in poplar [76]. In the current research, the expression level of *LrWRKY3* (homolog of *AtWRKY75*) was increased under drought stress, suggesting that *LrWRKY3* may participate in the drought stress response mechanism of *Lycoris* by regulating the activity of some hormone-like proteins and enhancing the *Lycoris* drought tolerance (Figure 6A). The overexpression of *AtWRKY8*, *AtWRKY28*, and *AtWRKY17* enhance drought or salt tolerance stress in *Arabidopsis* [27,77]. Similarly, the expression pattern of *LrWRKY11* (homolog of *AtWRKY8*, *AtWRKY28*, and *AtWRKY17*) can also be induced after drought treatment and interact with some regulatory factor or unknown binding protein to regulate the expression pattern of target genes, indicating that *LrWRKY11* plays an important role in drought stress tolerance in *L. radiata*. The expression level of *AtWRKY40* induces drought stress [78] and is consistent with the *LrWRKYs* expression dataset results, which showed that *LrWRKY13* (homolog of *AtWRKY40*) is involved in the drought stress response. *AtWRKY33* plays a critical role in broad plant stress responses in *Arabidopsis* [79], suggesting that drought stress induces *LrWRKY10* (homolog of *AtWRKY33*). Therefore, *LrWRKY3*, *LrWRKY10*, *LrWRKY11*, and *LrWRKY13* have played potential functions in the drought stress response. The results indicate that these genes potentially are involved in the drought resistance of *L. radiata*. Nonetheless, further experimental studies should be carried out to enunciate the accurate regulatory mechanism through which *LrWRKYs* respond to drought stress.

MeJA is an important regulator in plant growth, stress response, and secondary metabolism in both angiosperms and gymnosperms [80,81]. Many studies found that anthocyanin biosynthesis and many MeJA-responsive TFs are regulated by MeJA signaling pathway [82–85]. For example, *AtWRKY11* (homolog of *LrWRKY6*), *AtWRKY17*, and *AtWRKY70* (homolog of *LrWRKY21*) are essential components of the confrontational action in JA and the SA-mediated signaling pathway [28,86]. In addition, *WRKY75* (homolog of *LrWRKY3*) regulated the JA-mediated signaling pathway to modulate defense responses in *A. thaliana*. Under normal conditions, *WRKY75* interacted with Jasmonate ZIM domain (JAZ) protein to inhibit the JA signaling pathway [87]. *PpWRKY46* and *PpWRKY53* contribute to MeJA-primed defense by regulating the energy metabolism in peaches [88]. In tomato, *SIWRKY37* positively regulates jasmonic acid- and dark-induced leaf senescence [89]. This study used publicly available transcriptome data and qRT-PCR to study the *LrWRKY* gene expression under MeJA induction (Figure 6B and Figure S3). *LrWRKY10*, *LrWRKY11*, *LrWRKY14*, and *LrWRKY22* showed the same expression pattern and the expression levels of *LrWRKY6*, *LrWRKY12*, *LrWRKY18*, and *LrWRKY28* increased significantly at 6 h under MeJA treatment. In summary, our findings provide a valuable resource for select candidate *LrWRKY* genes, which can facilitate the further functional studies of *LrWRKYs* involved in various biological stresses.

3.3. *LrWRKYs* Are Related to *L. radiata* Petal Color Change

Anthocyanins are among the key metabolites of petal color formation in plants, which have antioxidant, antiaging, and anti-inflammatory functions; the anthocyanin biosynthesis pathway has been widely investigated in many plants [90–92]. Previous studies have demonstrated that anthocyanin regulated the plant petal color formation and influenced pigmentation [93,94]. It has been shown that six anthocyanins (cyanidin, delphinidin, malvidin, pelargonidin, peonidin, and petunidin) are common in petal color changes [95,96]. In our research, 18 differential anthocyanins were identified in the *L. radiata* petals and mainly contained three categories of cyanidin, peonidin, and pelargonidin (Figure 7A). Additionally, most anthocyanin compounds showed significantly high expressions in the red petals; pelargonidin (pelargonidin-3-O-glucoside-5-O-arabinoside) may especially be the main source of red petal formation. Similar results have also been acknowledged in previous academic studies [95–97]. Furthermore, some key structural genes (such as *DFR*, *4CL*, *CHI*, *ANS*, *CHS*, and *F3'H*) involved in anthocyanin biosynthesis were also found based on RNA-seq profiling and were significantly up-regulated, indicating that WRKY TFs have a greater effect on anthocyanin [53].

In recent years, many studies have investigated the conservation of WRKY-based regulatory mechanisms in the anthocyanin biosynthesis pathway, such as in *Arabidopsis*, in which WRKY TFs combined with the MBW (MYB-bHLH-WD40) complex to regulate the anthocyanin biosynthesis pathway and control flavonoid pigment pathways [98,99]. In addition, WRKY was found to be involved in rhododendron color formation [100]. These studies illustrate that WRKY TFs play an important role in the pigment pathway. In our research, *LrWRKY3* showed that significantly different expression levels in petals might be candidate regulators of anthocyanin accumulation in petal color changes in *L. radiata* (Figures 7 and 8). The gene—metabolite correlation network showed that the metabolite pelargonidin-3-O-glucoside-5-O-arabinoside was strongly correlated with *LrWRKY3* in the anthocyanin biosynthesis pathways (Figure 7). Interestingly, our results also showed that the *LrWRKY3* transcription factor specifically interacted with the *ANR* and *LAR* gene, suggesting that it is involved in petal coloration in *L. radiata* (Figure 8). The WRKY transcription factors participate in the synthesis of anthocyanins across a diversity of different species; therefore, more research is needed to understand how WRKY has evolved throughout angiosperms and what function it serves in other lineages.

4. Materials and Methods

4.1. Plant Materials and Plant Treatments

Lycoris radiata (L'Her.) Herb. was planted in the Experimental Plantation of the Institute of Botany, Jiangsu Province and the Chinese Academy of Sciences, Nanjing, China. The seedlings with the same or similar sizes (2.8–3.2 cm) in diameter were transferred into plastic pots with a mixture of vermiculite and soil (1:1, v/v) and maintained in a plant growth chamber under the following conditions: 16 h light/8 h dark cycle at 25 °C/22 °C and 120 $\mu\text{mol m}^{-2} \text{s}^{-1}$ irradiation). After one week of maintenance, the seedlings were subjected to 100 $\mu\text{mol L}^{-1}$ methyl jasmonate (MeJA) for 0 h, 6 h, 12 h, 24 h, and 36 h and drought stress (20% PEG6000) for 24 h. Each treatment was replicated three times. The tissue-specific transcription profiles of the *LrWRKY* genes were explored in the petals, flower-stalks, gynoeciums, stamens, leaves, seeds, roots, and bulbs of these plants. All the samples were immediately frozen in liquid nitrogen and stored at -80 °C.

4.2. Transcriptome-Wide Identification and Expression Profiling of *LrWRKY* Genes

The *L. radiata* transcriptome database during the four flower development stages with 87,584 unigenes was used for potential *LrWRKY* searching [53]. The AtWRKY proteins downloaded from TAIR (Arabidopsis Information Resource database, <https://www.arabidopsis.org/> (accessed on 20 September 2022)) were utilized to determine the sequence homology with *L. radiata* transcripts from the database using basic local alignment (BLASTn). The hidden Markov model (HMM) profile of the WRKY DNA binding domain (PF03106) obtained from the

Pfam protein family database (<http://pfam.xfam.org> (accessed on 20 September 2022)) [101] was used to search candidate *LrWRKY* genes. Then, we verified the WRKY domain in the predicted *LrWRKY* transcription factors utilizing the NCBI Batch CD-Search Tool (<https://www.ncbi.nlm.nih.gov/Structure/bwrpsb/bwrpsb.cgi> (accessed on 20 September 2022)) with default parameters. This characteristic was deemed to have a high-confidence association with the conserved domain. The sequences predicted as specific hits were retained for further analysis (Table S4). Furthermore, the PFAM and SMART (<http://smart.embl-heidelberg.de/> (accessed on 20 September 2022)); [102] databases were used for verifying the WRKY domain in all the candidate protein sequences. Finally, the ExPASy website (<https://web.expasy.org/protparam> (accessed on 20 September 2022)) [103] was utilized to determine the full length of the amino acid sequences, isoelectric points (PI), molecular sizes (MW), and protein instability index.

4.3. Phylogenetic Tree and Protein Motif Analyses of *LrWRKY* Proteins

The phylogenetic tree of WRKYs from *L. radiata* and *A. thaliana* was constructed with MEGA7 using the neighbor-joining method (<https://www.megasoftware.net/> (accessed on 20 September 2022)). The *LrWRKY* proteins were then classified according to their phylogenetic relationships with AtWRKY proteins. The online tool MEME (Multiple EM for Motif Elicitation, version 5.1.1) was utilized to search for the conserved motifs of *LrWRKY* proteins (<https://meme-suite.org/meme/tools/meme>; [104] (accessed on 20 September 2022)), with the motif number and a width of 21–50 for each gene. The motifs were also searched in protein databases using the SMART program (<http://smart.embl.de/> (accessed on 20 September 2022)).

4.4. Gene Ontology Annotation of *LrWRKYs*

The Gene Ontology (GO) functional annotations were conducted using KOBAS. The top 20 functional terms for credibility in the three categories (biological processes, cellular components, and molecular function) were selected for visualization.

4.5. Expression Profiles Analysis and Real-Time Quantitative PCR Analysis of *LrWRKYs* Genes

The RNA-seq data for the *LrWRKY* genes were obtained from previous studies on gene expression in different flower developmental stages and MeJA treatment [53,54]. The *LrWRKY* gene expression profiles were evaluated utilizing the values of FPKM. TBtools [105] software was utilized to generate *LrWRKYs* expression heatmaps. The total RNA was extracted using an RNA prep Pure Plant Kit (Cat BC508, Huayueyang, Beijing, China) according to the manufacturer's protocol. The cDNA was synthesized by using a Prime-Script™ II 1st Strand cDNA Synthesis Kit (Takara Bio, Dalian, China) and utilized for qRT-PCR assays. The relative expression levels of the genes were analyzed using qRT-PCR with SYBR® Premix Ex Taq™ II (Takara Bio, Dalian, China) on a Bio-Rad iQ5 Real-Time PCR System (Bio-Rad, Hercules, CA, USA) in 15 µL reactions. Each reaction contained 7.5 µL 2 × TransStart® Top Green qPCR SuperMix, 5.9 µL ddH₂O, 1 µL cDNA, and 0.6 µL of 10 µM forward and reverse primers, and 6.2 µL of ddH₂O. The RT-qPCR protocol included the following: the PCR reaction conditions were at 95 °C for 5 min; denaturation 5 s at 95 °C; 60 °C for 30 s; and 40 cycles. The *LrTIP41* gene was utilized as an endogenous control to normalize the relative expression levels based on the $2^{-\Delta\Delta C_t}$ method [106]. The specific primer sequences used in this research are listed in Supplementary Table S6.

4.6. Genes Gene Cloning and Construction of Expression Vectors

The *LrWRKYs* were cloned based on putative ORFs of unigenes from the RNA-seq database. The primers were synthesized for ORF sequence amplification using Tks Gflex™ DNA Polymerase (Takara, Dalian, China) from *L. radiata* petal cDNA (Table S6). The reaction conditions were: 3 min of 95 °C, 40 cycles for 30 s at 94 °C, 30 s at 58 °C, 2 min at 72 °C, and with extension at 72 °C for 10 min. The PCR products were cloned into pTOPO001 simple vectors (Genesand, Beijing, China). Afterward, those T-vectors were transferred into TOP10 competent cells (Genesand, Beijing, China) for amplification. The *LrWRKYs*

overexpression vectors were built by linking their ORFs into a pBIN-MCS-GFP4 plant transformation vector by using the One Step Cloning Kit (Genesand, Beijing, China). Then, the 35S:LrWRKYs recombinant vectors were transformed into *Agrobacterium tumefaciens* GV3101 competent cells.

4.7. Anthocyanin Quantification and Data Analysis of *L. radiata*

The metabolite data acquisition was conducted with a UPLC-ESI-MS/MS system (Shim-pack UFLC SHIMADZU Nexera X2) (ultrafast liquid chromatography) instrument coupled to an MS/MS (Applied Biosystems 4500 QTRAP). The chromatographic separation was carried out on a Waters ACQUITY UPLC HSS T3 system (Shim-pack UFLC SHIMADZU CBM30A, see text footnote 2), which was equipped with a C18 column (1.8 mm × 2.1 mm × 100 mm), at 40 °C. The injection volume was 5 mL at a flow rate of 0.4 mL/min. The organic phase was acetonitrile (0.1% formic acid) and the mobile phase was ultrapure water (0.1% formic acid). The elution gradient was as follows: 0 min, 95:5 water/acetonitrile (*v/v*); 9.0 min, 5:95 water/acetonitrile; 10.0 min, 5:95 water/acetonitrile; 11.1 min, 95:5 water/acetonitrile; and 14.0 min, 95:5 water/acetonitrile. The metabolites eluted from the HPLC were monitored for each period using scheduled multiple reaction monitoring (MRM). The MRM signals were transformed and analyzed using the Analyst 1.6.3 software (Metware Biotechnology Co., Ltd., Wuhan, China). The metabolite identification and quantification were conducted following the commercially available standard Metabolites Database [107] (Metware Biotechnology Co., Ltd., Wuhan, China) and public metabolite databases [108]. The transcriptional regulatory networks were generated by combining the Pearson correlation coefficient ($|PCC| > 0.8$ or $|PCC| > 0.9$) between structural genes and transcription factors and anthocyanins metabolites. Finally, the regulatory network maps were visualized by Cytoscape (v.3.7.2, Seattle, WA, USA).

4.8. Subcellular Localization Analysis of LrWRKY Proteins

The subcellular localization of LrWRKY proteins was predicted using WolfPsort (<https://wolfsort.hgc.jp> (accessed on 20 September 2022); [109]), ProtComp 9.0 (<http://linux1.softberry.com> (accessed on 20 September 2022)), and Plant-mPLOC (<http://www.csbio.sjtu.edu.cn/bioinf/plant-multi/> (accessed on 20 September 2022)). The coding regions of each LrWRKY gene were inserted into the pBinGFP4 plant expression vector. This vector was then used to transform *A. tumefaciens* strain GV3101 bacteria. The recombinant *A. tumefaciens* strains that contained various constructs were cultivated, harvested, followed by resuspension in an invasive solution (10 mM MES, 0.2 mM Acetosyringone, and 10 mM MgCl₂) with a final OD₆₀₀ value of 0.6. Forty-day-old *N. benthamiana* plants were used for infiltration. After infiltration, the plants were grown at 22 °C in the dark and then transferred to normal growth conditions (25 °C/16 h light and 22 °C/8 h dark cycle) for three days. The GFP fluorescent signals in the epidermal cells of *N. benthamiana* leaves were observed under a confocal microscope (Zeiss LSM900, Jena, Germany).

4.9. PPI Network Prediction of LrWRKY Proteins

The potential protein–protein interaction networks were predicted using the STRING online database (version 11.5) based on *A. thaliana* homologous proteins (<https://cn.string-db.org> (accessed on 20 September 2022); [110]). The protein sequences of 31 LrWRKYs (Table S4) were uploaded into the server selecting *A. thaliana* as the comparative organism. The LrWRKY gene interaction network was constructed after blasting with the highest bitscore.

4.10. Statistical Analysis

All the experiments were independently duplicated at least three times. The results were represented as mean ± SD of biological triplicates. The student *t*-test was utilized for data analysis. * $p < 0.05$ and ** $p < 0.01$ were regarded significant.

5. Conclusions

In this study, 31 *LrWRKY* genes were identified from the transcriptome of *L. radiata* and enriched by systematically analyzing the basic biochemical information, phylogenetic relationships, conserved motifs, and gene expression profiling. Most *LrWRKY* genes were revealed to likely play various important roles in *Lycoris* growth and development, especially in flower development stages. The analysis of the expression pattern of *LrWRKY* genes in response to drought stress and MeJA treatment suggested that the *LrWRKY* genes could be importantly involved in drought stress as well as in JA signaling pathway. The gene—metabolite correlation network analysis revealed a potential regulatory role of *LrWRKYs* in anthocyanin biosynthetic pathway. A PPI analysis of *LrWRKY* proteins was performed to explore the functions and regulatory mechanisms in *L. radiata*. In conclusion, this study provides valuable information for further research on the regulatory mechanisms of WRKY TFs in plant growth, secondary metabolism, and resistance to various stressors.

Supplementary Materials: The following supporting information can be downloaded at: <https://www.mdpi.com/article/10.3390/ijms24032423/s1>.

Author Contributions: N.W. and Z.W. were major contributors in writing the manuscript. G.S., X.S., F.Z. and G.C. contributed to plant sample collection, DNA/RNA preparation, library construction, and sequencing. W.Z., T.W. and Y.L. worked on gene assembly and annotation. N.W. and Z.W. conducted transcriptome analysis and identified functional genes involved in petal color formation. N.W. and Z.W. analyzed the gene family and constructed the evolutionary tree. Z.W. conceived of the study, participated in its design and data interpretation, and revised the manuscript critically. All authors contributed to the article and approved the submitted version. All authors have read and agreed to the published version of the manuscript.

Funding: This research was financially supported by the Jiangsu Key Laboratory for the Research and Utilization of Plant Resources (Grant No. JSPKLB202020); Jiangsu Agricultural Science and Technology Innovation Fund (Grand No. CX(20)3171); Jiangsu Provincial Crop Germplasm Resource Bank for Conservation (Grand No. 2022-SJ-015); and Projects of Independently Development of Jiangsu Provincial Department of Science and Technology (Grand No. BM2018021-5).

Institutional Review Board Statement: Not applicable.

Informed Consent Statement: Not applicable.

Data Availability Statement: All data are displayed in the manuscript.

Conflicts of Interest: The authors declare no conflict of interest.

References

- Javed, T.; Shabbir, R.; Ali, A.; Afzal, I.; Zaheer, U.; Gao, S.J. Transcription factors in plant stress responses: Challenges and potential for Sugarcane improvement. *Plants* **2020**, *9*, 491. [\[CrossRef\]](#) [\[PubMed\]](#)
- Romani, F.; Moreno, J.E. Molecular mechanisms involved in functional macroevolution of plant transcription factors. *New Phytol.* **2021**, *230*, 1345–1353. [\[CrossRef\]](#) [\[PubMed\]](#)
- Wani, S.H.; Anand, S.; Singh, B.; Bohra, A.; Joshi, R. WRKY transcription factors and plant defense responses: Latest discoveries and future prospects. *Plant Cell Rep.* **2021**, *40*, 1071–1085. [\[CrossRef\]](#) [\[PubMed\]](#)
- Javed, T.; Zhou, J.R.; Li, J.; Hu, Z.T.; Wang, Q.N.; Gao, S.J. Identification and expression profiling of WRKY family genes in sugarcane in response to bacterial pathogen infection and nitrogen implantation dosage. *Front. Plant Sci.* **2022**, *13*, 917953. [\[CrossRef\]](#)
- Rushton, P.J.; Somssich, I.E.; Ringler, P.; Shen, Q.J. WRKY transcription factors. *Trends Plant Sci.* **2010**, *15*, 247–258. [\[CrossRef\]](#) [\[PubMed\]](#)
- Zhu, H.; Jiang, Y.; Guo, Y.; Huang, J.; Zhou, M.; Tang, Y.; Sui, J.; Wang, J.; Qiao, L. A novel salt inducible WRKY transcription factor gene, AhWRKY75, confers salt tolerance in transgenic peanut. *Plant Physiol. Biochem.* **2021**, *160*, 175–183. [\[CrossRef\]](#) [\[PubMed\]](#)
- Li, Z.; Hua, X.; Zhong, W.; Yuan, Y.; Wang, Y.; Wang, Z.; Ming, R.; Zhang, J. Genome-wide identification and expression profile analysis of WRKY family genes in the autoployploid *Saccharum spontaneum*. *Plant Cell Physiol.* **2020**, *61*, 616–630. [\[CrossRef\]](#)
- Zhang, Y.; Wang, L. The WRKY transcription factor superfamily: Its origin in eukaryotes and expansion in plants. *BMC Evol. Biol.* **2005**, *5*, 1. [\[CrossRef\]](#) [\[PubMed\]](#)
- Chen, X.; Chen, R.; Wang, Y.; Wu, C.; Huang, J. Genome-wide identification of WRKY transcription factors in Chinese jujube (*Ziziphus jujuba* Mill.) and their involvement in fruit developing, ripening, and abiotic stress. *Genes* **2019**, *10*, 360. [\[CrossRef\]](#)

10. Eulgem, T.; Rushton, P.J.; Robatzek, S.; Somssich, I.E. The WRKY superfamily of plant transcription factors. *Trends Plant Sci.* **2000**, *5*, 199–206. [[CrossRef](#)]
11. Dong, J.; Chen, C.; Chen, Z. Expression profiles of the *Arabidopsis* WRKY gene superfamily during plant defense response. *Plant Mol. Biol.* **2003**, *51*, 21–37. [[CrossRef](#)] [[PubMed](#)]
12. He, Y.; Mao, S.; Gao, Y.; Zhu, L.; Wu, D.; Cui, Y.; Li, J.; Qian, W. Genome-wide identification and expression analysis of WRKY transcription factors under multiple stresses in *Brassica napus*. *PLoS ONE* **2016**, *11*, e0157558. [[CrossRef](#)] [[PubMed](#)]
13. Wu, J.; Chen, J.; Wang, L.; Wang, S. Genome-wide investigation of WRKY transcription factors involved in terminal drought stress response in common bean. *Front. Plant Sci.* **2017**, *8*, 380. [[CrossRef](#)] [[PubMed](#)]
14. Xie, T.; Chen, C.; Li, C.; Liu, J.; Liu, C.; He, Y. Genome-wide investigation of WRKY gene family in pineapple: Evolution and expression profiles during development and stress. *BMC Genom.* **2018**, *19*, 490. [[CrossRef](#)] [[PubMed](#)]
15. Baillo, E.H.; Hanif, M.S.; Guo, Y.; Zhang, Z.; Xu, P.; Algam, S.A. Genome-wide identification of WRKY transcription factor family members in sorghum (*Sorghum bicolor* (L.) moench). *PLoS ONE* **2020**, *15*, e0236651. [[CrossRef](#)] [[PubMed](#)]
16. Wu, W.; Zhu, S.; Xu, L.; Zhu, L.; Wang, D.; Liu, Y.; Liu, S.; Hao, Z.; Lu, Y.; Yang, L.; et al. Genome-wide identification of the *Liriodendron chinense* WRKY gene family and its diverse roles in response to multiple abiotic stress. *BMC Plant Biol.* **2022**, *22*, 25. [[CrossRef](#)]
17. Ayoub Khan, M.; Dongru, K.; Yifei, W.; Ying, W.; Penghui, A.; Zicheng, W. Characterization of WRKY gene family in whole-genome and exploration of flowering improvement genes in *Chrysanthemum lavandulifolium*. *Front. Plant Sci.* **2022**, *13*, 861193. [[CrossRef](#)]
18. Yan, L.; Jin, H.; Raza, A.; Huang, Y.; Gu, D.; Zou, X. WRKY genes provide novel insights into their role against *Ralstonia solanacearum* infection in cultivated peanut (*Arachis hypogaea* L.). *Front. Plant Sci.* **2022**, *13*, 986673. [[CrossRef](#)]
19. Phukan, U.J.; Jeena, G.S.; Shukla, R.K. WRKY transcription factors: Molecular regulation and stress responses in plants. *Front. Plant Sci.* **2016**, *7*, 760. [[CrossRef](#)]
20. Jiang, J.; Ma, S.; Ye, N.; Jiang, M.; Cao, J.; Zhang, J. WRKY transcription factors in plant responses to stresses. *J. Integr. Plant Biol.* **2017**, *59*, 86–101. [[CrossRef](#)]
21. Li, W.; Pang, S.; Lu, Z.; Jin, B. Function and mechanism of WRKY transcription factors in abiotic stress responses of plants. *Plants* **2020**, *9*, 1515. [[CrossRef](#)] [[PubMed](#)]
22. Wang, J.; Wang, L.; Yan, Y.; Zhang, S.; Li, H.; Gao, Z.; Wang, C.; Guo, X. GhWRKY21 regulates ABA-mediated drought tolerance by fine-tuning the expression of GhHAB in cotton. *Plant Cell Rep.* **2021**, *40*, 2135–2150. [[CrossRef](#)] [[PubMed](#)]
23. Gao, H.; Wang, Y.; Xu, P.; Zhang, Z. Overexpression of a WRKY transcription factor TaWRKY2 enhances drought stress tolerance in transgenic wheat. *Front. Plant Sci.* **2018**, *9*, 997. [[CrossRef](#)] [[PubMed](#)]
24. Ren, X.; Chen, Z.; Liu, Y.; Zhang, H.; Zhang, M.; Liu, Q.; Hong, X.; Zhu, J.K.; Gong, Z. ABO3, a WRKY transcription factor, mediates plant responses to abscisic acid and drought tolerance in *Arabidopsis*. *Plant J.* **2010**, *63*, 417–429. [[CrossRef](#)]
25. El-Esawi, M.A.; Al-Ghamdi, A.A.; Ali, H.M.; Ahmad, M. Overexpression of AtWRKY30 transcription factor enhances heat and drought stress tolerance in wheat (*Triticum aestivum* L.). *Genes* **2019**, *10*, 163. [[CrossRef](#)]
26. Ali, M.A.; Azeem, F.; Nawaz, M.A.; Acet, T.; Abbas, A.; Imran, Q.M.; Shah, K.H.; Rehman, H.M.; Chung, G.; Yang, S.H.; et al. Transcription factors WRKY11 and WRKY17 are involved in abiotic stress responses in *Arabidopsis*. *J. Plant Physiol.* **2018**, *226*, 12–21. [[CrossRef](#)]
27. Babitha, K.C.; Ramu, S.V.; Pruthvi, V.; Mahesh, P.; Nataraja, K.N.; Udayakumar, M. Co-expression of AtbHLH17 and AtWRKY28 confers resistance to abiotic stress in *Arabidopsis*. *Transg. Res.* **2013**, *22*, 327–341. [[CrossRef](#)]
28. Chen, J.N.; Nolan, T.M.; Ye, H.X.; Zhang, M.C.; Tong, H.N.; Xin, P.Y.; Chu, J.F.; Chu, C.C.; Li, Z.H.; Yin, Y.H. *Arabidopsis* WRKY46, WRKY54, and WRKY70 transcription factors are involved in brassinosteroid-regulated plant growth and drought responses. *Plant Cell* **2017**, *29*, 1425–1439. [[CrossRef](#)]
29. Ma, J.; Gao, X.; Liu, Q.; Shao, Y.; Zhang, D.; Jiang, L.; Li, C. Overexpression of TaWRKY146 Increases drought tolerance through inducing stomatal closure in *Arabidopsis thaliana*. *Front. Plant Sci.* **2017**, *8*, 2036. [[CrossRef](#)]
30. Wang, C.T.; Ru, J.N.; Liu, Y.W.; Li, M.; Zhao, D.; Yang, J.F.; Fu, J.D.; Xu, Z.S. Maize WRKY transcription factor ZmWRKY106 confers drought and heat tolerance in transgenic plants. *Int. J. Mol. Sci.* **2018**, *19*, 3046. [[CrossRef](#)]
31. Hu, Q.; Ao, C.; Wang, X.; Wu, Y.; Du, X. GhWRKY1-like, a WRKY transcription factor, mediates drought tolerance in *Arabidopsis* via modulating ABA biosynthesis. *BMC Plant Biol.* **2021**, *21*, 458. [[CrossRef](#)] [[PubMed](#)]
32. Ye, H.; Qiao, L.Y.; Guo, H.Y.; Guo, L.P.; Ren, F.; Bai, J.F.; Wang, Y.K. Genome-wide identification of wheat WRKY gene family reveals that TaWRKY75-A is referred to drought and salt resistances. *Front. Plant Sci.* **2021**, *12*, 812. [[CrossRef](#)] [[PubMed](#)]
33. Lv, M.; Luo, W.; Ge, M.; Guan, Y.; Tang, Y.; Chen, W.; Lv, J. A group I WRKY Gene, TaWRKY133, negatively regulates drought resistance in transgenic plants. *Int. J. Mol. Sci.* **2022**, *23*, 12026. [[CrossRef](#)] [[PubMed](#)]
34. Zhang, J.; Huang, D.; Zhao, X.; Zhang, M.; Wang, Q.; Hou, X.; Di, D.; Su, B.; Wang, S.; Sun, P. Drought-responsive WRKY transcription factor genes IgWRKY50 and IgWRKY32 from *Iris germanica* enhance drought resistance in transgenic *Arabidopsis*. *Front. Plant Sci.* **2022**, *13*, 983600. [[CrossRef](#)]
35. Huang, Z.; Song, L.; Xiao, Y.; Zhong, X.; Wang, J.; Xu, W.; Jiang, C.Z. Overexpression of *Myrothamnus flabellifolia* MfWRKY41 confers drought and salinity tolerance by enhancing root system and antioxidation ability in *Arabidopsis*. *Front. Plant Sci.* **2022**, *13*, 967352. [[CrossRef](#)]

36. Song, G.; Son, S.; Lee, K.S.; Park, Y.J.; Suh, E.J.; Lee, S.I.; Park, S.R. OsWRKY114 negatively regulates drought tolerance by restricting stomatal closure in rice. *Plants* **2022**, *11*, 1938. [[CrossRef](#)]
37. Fan, C.; Yao, H.; Qiu, Z.; Ma, H.; Zeng, B. Genome-wide analysis of *Eucalyptus grandis* WRKY genes family and their expression profiling in response to hormone and abiotic stress treatment. *Gene* **2018**, *678*, 38–48. [[CrossRef](#)]
38. Jiang, Y.; Duan, Y.; Yin, J.; Ye, S.; Zhu, J.; Zhang, F.; Lu, W.; Fan, D.; Luo, K. Genome-wide identification and characterization of the *Populus* WRKY transcription factor family and analysis of their expression in response to biotic and abiotic stresses. *J. Exp. Bot.* **2014**, *65*, 6629–6644. [[CrossRef](#)]
39. Wang, L.; Liu, F.; Zhang, X.; Wang, W.; Sun, T.; Chen, Y.; Dai, M.; Yu, S.; Xu, L.; Su, Y.; et al. Expression characteristics and functional analysis of the ScWRKY3 gene from sugarcane. *Int. J. Mol. Sci.* **2018**, *19*, 4059. [[CrossRef](#)]
40. Wang, D.; Wang, L.; Su, W.; Ren, Y.; You, C.; Zhang, C.; Que, Y.; Su, Y. A class III WRKY transcription factor in sugarcane was involved in biotic and abiotic stress responses. *Sci. Rep.* **2020**, *10*, 20964. [[CrossRef](#)]
41. Kang, G.; Yan, D.; Chen, X.; Yang, L.; Zeng, R. HbWRKY82, a novel IIc WRKY transcription factor from *Hevea brasiliensis* associated with abiotic stress tolerance and leaf senescence in *Arabidopsis*. *Physiol. Plant.* **2021**, *171*, 151–160. [[CrossRef](#)] [[PubMed](#)]
42. Liu, W.; Wang, Y.; Yu, L.; Jiang, H.; Guo, Z.; Xu, H.; Jiang, S.; Fang, H.; Zhang, J.; Su, M.; et al. MdWRKY11 participates in anthocyanin accumulation in red-fleshed apples by affecting MYB transcription factors and the photoresponse factor MdHY5. *J. Agric. Food Chem.* **2019**, *67*, 8783–8793. [[CrossRef](#)] [[PubMed](#)]
43. Li, C.; Wu, J.; Hu, K.D.; Wei, S.W.; Sun, H.Y.; Hu, L.Y.; Han, Z.; Yao, G.F.; Zhang, H. PyWRKY26 and PybHLH3 cotargeted the PyMYB114 promoter to regulate anthocyanin biosynthesis and transport in red-skinned pears. *Hortic. Res.* **2020**, *7*, 37. [[CrossRef](#)]
44. Cong, L.; Qu, Y.; Sha, G.; Zhang, S.; Ma, Y.; Chen, M.; Zhai, R.; Yang, C.; Xu, L.; Wang, Z. PbWRKY75 promotes anthocyanin synthesis by activating PbDFR, PbUFGT, and PbMYB10b in pear. *Physiol. Plant.* **2021**, *173*, 1841–1849. [[CrossRef](#)]
45. Zhang, H.; Zhang, Z.; Zhao, Y.; Guo, D.; Zhao, X.; Gao, W.; Zhang, J.; Song, B. StWRKY13 promotes anthocyanin biosynthesis in potato (*Solanum tuberosum*) tubers. *Funct. Plant Biol.* **2021**, *49*, 102–114. [[CrossRef](#)]
46. Zhang, J.; Wang, Y.; Mao, Z.; Liu, W.; Ding, L.; Zhang, X.; Yang, Y.; Wu, S.; Chen, X.; Wang, Y. Transcription factor McWRKY71 induced by ozone stress regulates anthocyanin and proanthocyanidin biosynthesis in *Malus crabapple*. *Ecotoxicol. Environ. Saf.* **2022**, *232*, 113274. [[CrossRef](#)]
47. Su, M.; Zuo, W.; Wang, Y.; Liu, W.; Zhang, Z.; Wang, N.; Chen, X. The WKRY transcription factor MdWRKY75 regulates anthocyanins accumulation in apples (*Malus domestica*). *Funct. Plant Biol.* **2022**, *49*, 799–809. [[CrossRef](#)] [[PubMed](#)]
48. Cahliková, L.; Breiterová, K.; Opletal, L. Chemistry and biological activity of alkaloids from the genus *Lycoris* (*Amaryllidaceae*). *Molecules* **2020**, *5*, 4797. [[CrossRef](#)] [[PubMed](#)]
49. Jin, Z. Amaryllidaceae and scelletium alkaloids. *Nat. Prod. Rep.* **2011**, *28*, 1126–1142. [[CrossRef](#)] [[PubMed](#)]
50. Feng, T.; Wang, Y.Y.; Su, J.; Li, Y.; Cai, X.H.; Luo, X.D. Amaryllidaceae alkaloids from *Lycoris radiata*. *Helv. Chim. Acta* **2011**, *94*, 178–183. [[CrossRef](#)]
51. Chen, G.L.; Tian, Y.Q.; Wu, J.L.; Li, N.; Guo, M.Q. Antiproliferative activities of *Amaryllidaceae* alkaloids from *Lycoris radiata* targeting DNA topoisomerase I. *Sci. Rep.* **2016**, *6*, 38284. [[CrossRef](#)] [[PubMed](#)]
52. Shen, C.Y.; Xu, X.L.; Yang, L.J.; Jiang, J.G. Identification of narciclasine from *Lycoris radiata* (L'Her.) Herb. and its inhibitory effect on LPS-induced inflammatory responses in macrophages. *Food Chem. Toxicol.* **2019**, *125*, 605–613. [[CrossRef](#)] [[PubMed](#)]
53. Wang, N.; Shu, X.; Zhang, F.; Zhuang, W.; Wang, T.; Wang, Z. Comparative transcriptome analysis identifies key regulatory genes involved in anthocyanin metabolism during flower development in *Lycoris radiata*. *Front. Plant Sci.* **2021**, *12*, 761862. [[CrossRef](#)] [[PubMed](#)]
54. Wang, R.; Xu, S.; Wang, N.; Xia, B.; Jiang, Y.; Wang, R. Transcriptome analysis of secondary metabolism pathway, transcription factors, and transporters in response to methyl jasmonate in *Lycoris aurea*. *Front. Plant Sci.* **2017**, *7*, 1971. [[CrossRef](#)] [[PubMed](#)]
55. Park, C.H.; Yeo, H.J.; Park, Y.E.; Baek, S.A.; Kim, J.K.; Park, S.U. Transcriptome analysis and metabolic profiling of *Lycoris radiata*. *Biology* **2019**, *8*, 63. [[CrossRef](#)]
56. Yue, Y.; Liu, J.; Shi, T.; Chen, M.; Li, Y.; Du, J.; Jiang, H.; Yang, X.; Hu, H.; Wang, L. Integrating transcriptomic and GC-MS metabolomic analysis to characterize color and aroma formation during tepal development in *Lycoris longituba*. *Plants* **2019**, *8*, 53. [[CrossRef](#)]
57. Li, Q.; Xu, J.; Yang, L.; Zhou, X.; Cai, Y.; Zhang, Y. Transcriptome analysis of different tissues reveals key genes associated with galanthamine biosynthesis in *Lycoris longituba*. *Front. Plant Sci.* **2020**, *11*, 519752. [[CrossRef](#)]
58. Ren, Z.M.; Zhang, D.; Jiao, C.; Li, D.Q.; Wu, Y.; Wang, X.Y.; Gao, C.; Lin, Y.F.; Ruan, Y.L.; Xia, Y.P. Comparative transcriptome and metabolome analyses identified the mode of sucrose degradation as a metabolic marker for early vegetative propagation in bulbs of *Lycoris*. *Plant J.* **2022**, *112*, 115–134. [[CrossRef](#)]
59. Bakshi, M.; Oelmüller, R. WRKY transcription factors: Jack of many trades in plants. *Plant Signal. Behav.* **2014**, *9*, e27700. [[CrossRef](#)]
60. Zhao, N.; He, M.; Li, L.; Cui, S.; Hou, M.; Wang, L.; Mu, G.; Liu, L.; Yang, X. Identification and expression analysis of WRKY gene family under drought stress in peanut (*Arachis hypogaea* L.). *PLoS ONE* **2020**, *15*, e0231396. [[CrossRef](#)]
61. Cheng, W.; Jiang, Y.; Peng, J.; Guo, J.; Lin, M.; Jin, C.; Huang, J.; Tang, W.; Guan, D.; He, S. The transcriptional reprogramming and functional identification of WRKY family members in pepper's response to *Phytophthora capsici* infection. *BMC Plant Biol.* **2020**, *20*, 256. [[CrossRef](#)]

62. Abdullah-Zawawi, M.R.; Ahmad-Nizamuddin, N.F.; Govender, N.; Harun, S.; Mohd-Assaad, N.; Mohamed-Hussein, Z.A. Comparative genome-wide analysis of WRKY, MADS-box and MYB transcription factor families in *Arabidopsis* and rice. *Sci. Rep.* **2021**, *11*, 19678. [[CrossRef](#)] [[PubMed](#)]
63. Yan, J.; Yu, X.; Ma, W.; Sun, X.; Ge, Y.; Yue, X.; Han, J.; Zhao, J.; Lu, Y.; Liu, M. Genome-wide identification and expression analysis of WRKY family genes under soft rot in *Chinese cabbage*. *Front. Genet.* **2022**, *13*, 958769. [[CrossRef](#)] [[PubMed](#)]
64. Liu, G.; Zhang, D.; Zhao, T.; Yang, H.; Jiang, J.; Li, J.; Zhang, H.; Xu, X. Genome-wide analysis of the WRKY gene family unveil evolutionary history and expression characteristics in tomato and its wild relatives. *Front. Genet.* **2022**, *13*, 962975. [[CrossRef](#)] [[PubMed](#)]
65. Zhang, C.; Wang, W.; Wang, D.; Hu, S.; Zhang, Q.; Wang, Z.; Cui, L. Genome-wide identification and characterization of the WRKY gene family in *scutellaria baicalensis georgi* under diverse abiotic stress. *Int. J. Mol. Sci.* **2022**, *23*, 4225. [[CrossRef](#)] [[PubMed](#)]
66. Song, Y.; Cui, H.; Shi, Y.; Xue, J.; Ji, C.; Zhang, C.; Yuan, L.; Li, R. Genome-wide identification and functional characterization of the *Camelina sativa* WRKY gene family in response to abiotic stress. *BMC Genom.* **2020**, *21*, 786. [[CrossRef](#)] [[PubMed](#)]
67. Liu, L.; White, M.J.; MacRae, T.H. Transcription factors and their genes in higher plants functional domains, evolution and regulation. *Eur. J. Biochem.* **1999**, *262*, 247–257. [[CrossRef](#)]
68. Wei, Y.; Shi, H.; Xia, Z.; Tie, W.; Ding, Z.; Yan, Y.; Wang, W.; Hu, W.; Li, K. Genome-wide identification and expression analysis of the WRKY gene family in cassava. *Front. Plant Sci.* **2016**, *7*, 25. [[CrossRef](#)] [[PubMed](#)]
69. Xu, Y.H.; Sun, P.W.; Tang, X.L.; Gao, Z.H.; Zhang, Z.; Wei, J.H. Genome-wide analysis of WRKY transcription factors in *Aquilaria sinensis* (Lour.) Gilg. *Sci. Rep.* **2020**, *10*, 3018. [[CrossRef](#)]
70. Kim, J.; Lee, J.; Choi, J.P.; Park, I.; Yang, K.; Kim, M.K.; Lee, Y.H.; Nou, I.S.; Kim, D.S.; Min, S.R.; et al. Functional innovations of three chronological mesohexaploid *Brassica rapa* genomes. *BMC Genom.* **2014**, *15*, 606. [[CrossRef](#)]
71. Li, J.; Brader, G.; Palva, E.T. The WRKY70 transcription factor: A node of convergence for jasmonate-mediated and salicylate-mediated signals in plant defense. *Plant Cell* **2004**, *16*, 319–331. [[CrossRef](#)] [[PubMed](#)]
72. Devaiah, B.N.; Karthikeyan, A.S.; Raghothama, K.G. WRKY75 transcription factor is a modulator of phosphate acquisition and root development in *Arabidopsis*. *Plant Physiol.* **2007**, *143*, 1789–1801. [[CrossRef](#)]
73. Lei, R.; Li, X.; Ma, Z.; Lv, Y.; Hu, Y.; Yu, D. *Arabidopsis* WRKY2 and WRKY34 transcription factors interact with VQ20 protein to modulate pollen development and function. *Plant J.* **2017**, *91*, 962–976. [[CrossRef](#)] [[PubMed](#)]
74. Zhang, H.; Zhang, L.; Wu, S.; Chen, Y.; Yu, D.; Chen, L. AtWRKY75 positively regulates age-triggered leaf senescence through gibberellin pathway. *Plant Divers.* **2020**, *43*, 331–340. [[CrossRef](#)] [[PubMed](#)]
75. Guo, P.; Li, Z.; Huang, P.; Li, B.; Fang, S.; Chu, J.; Guo, H. A Tripartite amplification loop involving the transcription factor WRKY75, salicylic acid, and reactive oxygen species accelerates leaf senescence. *Plant Cell* **2017**, *29*, 2854–2870. [[CrossRef](#)] [[PubMed](#)]
76. Zhang, Y.; Yang, X.; Nvsvrot, T.; Huang, L.; Cai, G.; Ding, Y.; Ren, W.; Wang, N. The transcription factor WRKY75 regulates the development of adventitious roots, lateral buds and callus by modulating hydrogen peroxide content in poplar. *J. Exp. Bot.* **2022**, *73*, 1483–1498. [[CrossRef](#)]
77. Hu, Y.; Chen, L.; Wang, H.; Zhang, L.; Wang, F.; Yu, D. *Arabidopsis* transcription factor WRKY8 functions antagonistically with its interacting partner VQ9 to modulate salinity stress tolerance. *Plant J.* **2013**, *74*, 730–745. [[CrossRef](#)]
78. Chen, H.; Lai, Z.; Shi, J.; Xiao, Y.; Chen, Z.; Xu, X. Roles of *Arabidopsis* WRKY18, WRKY40 and WRKY60 transcription factors in plant responses to abscisic acid and abiotic stress. *BMC Plant Biol.* **2010**, *10*, 281. [[CrossRef](#)]
79. Zhou, J.; Wang, J.; Zheng, Z.; Fan, B.; Yu, J.Q.; Chen, Z. Characterization of the promoter and extended C-terminal domain of *Arabidopsis* WRKY33 and functional analysis of tomato WRKY33 homologues in plant stress responses. *J. Exp. Bot.* **2015**, *66*, 4567–4583. [[CrossRef](#)]
80. Wasternack, C. Jasmonates: An update on biosynthesis, signal transduction and action in plant stress response, growth and development. *Ann. Bot.* **2007**, *100*, 681–697. [[CrossRef](#)]
81. Pauwels, L.; Inzé, D.; Goossens, A. Jasmonate-inducible gene: What does it mean? *Trends Plant Sci.* **2009**, *14*, 87–91. [[CrossRef](#)] [[PubMed](#)]
82. Browse, J.; Pauwels, L.; Inzé, D.; Goossens, A. Jasmonate passes muster: A receptor and targets for the defense hormone. *Annu. Rev. Plant Biol.* **2009**, *60*, 183–205. [[CrossRef](#)] [[PubMed](#)]
83. Chang, L.; Wu, S.; Tian, L. Methyl jasmonate elicits distinctive hydrolyzable tannin, flavonoid, and phyto-oxylipin responses in pomegranate (*Punica granatum* L.) leaves. *Planta* **2021**, *254*, 89. [[CrossRef](#)] [[PubMed](#)]
84. Tang, T.; Zhou, H.; Wang, L.; Zhao, J.; Ma, L.; Ling, J.; Li, G.; Huang, W.; Li, P.; Zhang, Y. Post-harvest application of methyl jasmonate or prohydrojasmon affects color development and anthocyanins biosynthesis in peach by regulation of sucrose metabolism. *Front. Nutr.* **2022**, *9*, 871467. [[CrossRef](#)]
85. Zhou, W.; Shi, M.; Deng, C.; Lu, S.; Huang, F.; Wang, Y.; Kai, G. The methyl jasmonate-responsive transcription factor SmMYB1 promotes phenolic acid biosynthesis in *Salvia miltiorrhiza*. *Hortic. Res.* **2021**, *8*, 10. [[CrossRef](#)] [[PubMed](#)]
86. Journot-catalino, N.; Somssich, I.E.; Roby, D.; Kroj, T. The transcription factors WRKY11 and WRKY17 act as negative regulators of basal resistance in *Arabidopsis thaliana*. *Plant Cell* **2006**, *18*, 3289–3302. [[CrossRef](#)]
87. Chen, L.; Zhang, L.; Xiang, S.; Chen, Y.; Zhang, H.; Yu, D. The transcription factor WRKY75 positively regulates jasmonate-mediated plant defense to necrotrophic fungal pathogens. *J. Exp. Bot.* **2021**, *72*, 1473–1489. [[CrossRef](#)] [[PubMed](#)]

88. Ji, N.; Li, Y.; Wang, J.; Zuo, X.; Li, M.; Jin, P.; Zheng, Y. Interaction of PpWRKY46 and PpWRKY53 regulates energy metabolism in MeJA primed disease resistance of peach fruit. *Plant Physiol. Biochem.* **2022**, *171*, 157–168. [[CrossRef](#)] [[PubMed](#)]
89. Wang, Z.; Gao, M.; Li, Y.; Zhang, J.; Su, H.; Cao, M.; Liu, Z.; Zhang, X.; Zhao, B.; Guo, Y.D.; et al. The transcription factor SlWRKY37 positively regulates jasmonic acid- and dark-induced leaf senescence in tomato. *J. Exp. Bot.* **2022**, *73*, 6207–6225. [[CrossRef](#)]
90. Zhang, X.; Lin, S.; Peng, D.; Wu, Q.; Liao, X.; Xiang, K.; Wang, Z.; Tembrock, L.R.; Bendahmane, M.; Bao, M.; et al. Integrated multi-omic data and analyses reveal the pathways underlying key ornamental traits in carnation flowers. *Plant Biotechnol. J.* **2022**, *20*, 1182–1196. [[CrossRef](#)]
91. Shao, D.; Liang, Q.; Wang, X.; Zhu, Q.H.; Liu, F.; Li, Y.; Zhang, X.; Yang, Y.; Sun, J.; Xue, F. Comparative metabolome and transcriptome analysis of anthocyanin biosynthesis in white and pink petals of cotton (*Gossypium hirsutum* L.). *Int. J. Mol. Sci.* **2022**, *23*, 10137. [[CrossRef](#)] [[PubMed](#)]
92. Pal, L.; Dwivedi, V.; Gupta, S.K.; Saxena, S.; Pandey, A.; Chattopadhyay, D. Biochemical analysis of anthocyanin and proanthocyanidin and their regulation in determining chickpea flower and seed coat colours. *J. Exp. Bot.* **2022**, *73*, erac392. [[CrossRef](#)] [[PubMed](#)]
93. Jiang, H.; Li, Z.; Jiang, X.; Qin, Y. Comparison of metabolome and transcriptome of flavonoid biosynthesis in two colors of coreopsis tinctoria Nutt. *Front. Plant Sci.* **2022**, *13*, 810422. [[CrossRef](#)] [[PubMed](#)]
94. Li, Y.; Gao, R.; Zhang, J.; Wang, Y.; Kong, P.; Lu, K.; Adnan Liu, M.; Ao, F.; Zhao, C.; Wang, L.; et al. The biochemical and molecular investigation of flower color and scent sheds lights on further genetic modification of ornamental traits in *Clivia miniata*. *Hortic. Res.* **2022**, *9*, uhac114. [[CrossRef](#)]
95. Xing, A.; Wang, X.; Nazir, M.F.; Zhang, X.; Wang, X.; Yang, R.; Chen, B.; Fu, G.; Wang, J.; Ge, H.; et al. Transcriptomic and metabolomic profiling of flavonoid biosynthesis provides novel insights into petals coloration in Asian cotton (*Gossypium arboreum* L.). *BMC Plant Biol.* **2022**, *22*, 416. [[CrossRef](#)]
96. Wang, X.; Li, L.; Liu, C.; Zhang, M.; Wen, Y. An integrated metabolome and transcriptome analysis of the *Hibiscus syriacus* L. petals reveal the molecular mechanisms of anthocyanin accumulation. *Front. Genet.* **2022**, *13*, 995748. [[CrossRef](#)]
97. Sun, X.; He, L.; Guo, Z.; Xiao, Z.; Su, J.; Liu, X.; Zhou, H.; Li, C.; Gao, H. Comparative transcriptome analyses reveal genes related to pigmentation in the petals of a flower color variation cultivar of *Rhododendron obtusum*. *Mol. Biol. Rep.* **2022**, *49*, 2641–2653. [[CrossRef](#)]
98. Verweij, W.; Spelt, C.E.; Bliiek, M.; de Vries, M.; Wit, N.; Faraco, M.; Koes, R.; Quattrocchio, F.M. Functionally similar WRKY proteins regulate vacuolar acidification in petunia and hair development in *Arabidopsis*. *Plant Cell* **2016**, *28*, 786–803. [[CrossRef](#)]
99. Lloyd, A.; Brockman, A.; Aguirre, L.; Campbell, A.; Bean, A.; Cantero, A.; Gonzalez, A. Advances in the MYB-bHLH-WD repeat (MBW) pigment regulatory model: Addition of a WRKY factor and co-option of an anthocyanin MYB for betalain regulation. *Plant Cell Physiol.* **2017**, *58*, 1431–1441. [[CrossRef](#)]
100. Yang, F.S.; Nie, S.; Liu, H.; Shi, T.L.; Tian, X.C.; Zhou, S.S.; Bao, Y.T.; Jia, K.H.; Guo, J.F.; Zhao, W.; et al. Chromosome-level genome assembly of a parent species of widely cultivated azaleas. *Nat. Commun.* **2020**, *11*, 5269. [[CrossRef](#)]
101. Mistry, J.; Chuguransky, S.; Williams, L.; Qureshi, M.; Salazar, G.A.; Sonnhammer, E.L.L.; Tosatto, S.C.E.; Paladin, L.; Raj, S.; Richardson, L.J.; et al. Pfam: The protein families database in 2021. *Nucleic Acids Res.* **2021**, *49*, D412–D419. [[CrossRef](#)] [[PubMed](#)]
102. Letunic, I.; Khedkar, S.; Bork, P. SMART: Recent updates, new developments and status in 2020. *Nucleic Acids Res.* **2021**, *49*, D458–D460. [[CrossRef](#)] [[PubMed](#)]
103. Artimo, P.; Jonnalagedda, M.; Arnold, K.; Baratin, D.; Csardi, G.; De Castro, E.; Duvaud, S.; Flegel, V.; Fortier, A.; Gasteiger, E.; et al. ExPASy: SIB bioinformatics resource portal. *Nucleic Acids Res.* **2012**, *40*, W597–W603. [[CrossRef](#)] [[PubMed](#)]
104. Bailey, T.L.; Johnson, J.; Grant, C.E.; Noble, W.S. The MEME suite. *Nucleic Acids Res.* **2015**, *43*, W39–W49. [[CrossRef](#)] [[PubMed](#)]
105. Chen, C.J.; Chen, H.; Zhang, Y.; Thomas, H.R.; Frank, M.H.; He, Y.; Xia, R. TBtools: An integrative toolkit developed for interactive analyses of big biological data. *Mol. Plant* **2020**, *13*, 1194–1202. [[CrossRef](#)]
106. Schmittgen, T.D.; Livak, K.J. Analyzing real-time PCR data by the comparative C(T) method. *Nat. Protoc.* **2008**, *3*, 1101–1108. [[CrossRef](#)] [[PubMed](#)]
107. Fu, M.; Yang, X.; Zheng, J.; Wang, L.; Yang, X.; Tu, Y.; Ye, J.; Zhang, W.; Liao, Y.; Cheng, S.; et al. Unraveling the regulatory mechanism of color diversity in camellia japonica petals by integrative transcriptome and metabolome analysis. *Front. Plant Sci.* **2021**, *12*, 685136. [[CrossRef](#)]
108. Wishart, D.S.; Guo, A.; Oler, E.; Wang, F.; Anjum, A.; Peters, H.; Dizon, R.; Sayeeda, Z.; Tian, S.; Lee, B.L.; et al. HMDB 5.0: The human metabolome database for 2022. *Nucleic Acids Res.* **2022**, *50*, D622–D631. [[CrossRef](#)]
109. Horton, P.; Park, K.J.; Obayashi, T.; Fujita, N.; Harada, H.; Adams-Collier, C.J.; Nakai, K. WoLF PSORT: Protein localization predictor. *Nucleic Acids Res.* **2007**, *35*, W585–W587. [[CrossRef](#)]
110. Szklarczyk, D.; Kirsch, R.; Koutrouli, M.; Nastou, K.; Mehryary, F.; Hachilif, R.; Gable, A.L.; Fang, T.; Doncheva, N.T.; Pyysalo, S.; et al. The STRING database in 2023: Protein-protein association networks and functional enrichment analyses for any sequenced genome of interest. *Nucleic Acids Res.* **2022**, *12*, gkac1000. [[CrossRef](#)]

Disclaimer/Publisher’s Note: The statements, opinions and data contained in all publications are solely those of the individual author(s) and contributor(s) and not of MDPI and/or the editor(s). MDPI and/or the editor(s) disclaim responsibility for any injury to people or property resulting from any ideas, methods, instructions or products referred to in the content.